IMPERIAL COLLEGE LONDON

Department of Earth Science and Engineering

Centre for Petroleum Studies

Carbon Dioxide Enhanced Oil Recovery

By

Abdul Rafay Zafar

A report submitted in partial fulfilment of the requirements for the MSc and/or the DIC.

September 2014

DECLARATION OF OWN WORK

I declare that this thesis

Carbon Dioxide Enhanced Oil Recovery

is entirely my own work and that where any material could be construed as the work of others, it is fully cited and referenced, and/or with appropriate acknowledgement given.

Signature:.....

Name of student: Abdul Rafay Zafar

Name of supervisor: Professor Martin J. Blunt

Name of the company supervisor: Marie-Ann Giddins

Abstract

This paper examines the impact of carbon dioxide (CO_2) dissolution in water for miscible carbon dioxide enhanced oil recovery (CO_2-EOR) and sequestration projects. In this study CO_2 water alternating gas (WAG) and simulations water alternating gas injection (SWAG) strategies is analysed on a simple synthetic homogenous and heterogeneous sector model.

A volatile 7-component compositional fluid model was used for the analysis. A 1D slimtube simulation was conducted, which determined the minimum miscibility pressure (MMP) for CO_2 injection. For this study we used a synthetic realistic three-phase permeability model using Oak's three-phase relative permeability curve end points (Oak, 1991) and to demonstrate three-phase WAG hysteresis effects using Larsen and Skauge (1998) model.

This paper concludes by discussing the effects of CO_2 solubility in CO_2 water alternating gas injection (WAG) and simultaneous water alternating gas injection (SWAG). We demonstrated the significance of including CO_2 solubility in water to quantify potential CO_2 injectivity losses in CO_2 –WAG strategies. We also demonstrate advantages of implementing CO_2 – SWAG injection in heterogeneous reservoir to maximize oil recovery. Depending on the project objective (1) maximizing oil recovery we recommend CO_2-SWAG injection (2) CO_2-EOR and sequestration CO_2-WAG is recommended. For CO_2-WAG simulations we propose to incorporate three-phase relative permeability hysteresis effects in conjunction with CO_2 solubility effects in water.

Acknowledgements

I am very thankful to Marie Ann Giddins (Schlumberger) for her support and inspiration for this project. I would also like to thank Professor Martin Blunt (Imperial College London) for his guidance.

Also, I would like to express my gratitude to all employees here in the Abingdon Technology Centre who shared their invaluable experience with me. I would like to thank Alan Thompson, Belraj Grewal and Samad Ali.

I am glad that my friends Bhavik, Sam, Mohsin, Oliver, Louis and Mansour were here with me in Abingdon.

Finally, I would like to thank my parents for their motivation and support throughout this project.

Table of Contents

Abstract 1
Introduction 1
Relative Permeability Hysteresis 2
Land trapping model 2
Larsen and Skauge Three-Phase Hysteresis model 3
Methodology 4
Relative Permeability Curves 4
Fluid Model 4
Homogenous model description 5
Injection Strategy and Pattern 5
Heterogeneous model description 6
Results and Analysis 7
Grid sensitivity study for compositional simulations 7
Effectiveness of injection patterns 7
Small scale CO_2 solubility and trapping effects 8
Macroscopic effects of CO_2 solubility 10
Impact of CO_2 solubility for different WAG Ratio 11
CO_2 –SWAG injection 11
Coupled CO_2-EOR and CO_2 sequestration 13
Heterogeneous application 14
Discussion 14
Conclusion 15
Recommendations for future study 15
Nomenclature 15
Reference 16
Appendix A: Literature Review 17
Appendix B: Fluid Model 36
Appendix C: Heterogenous model 37
Appendix D: ECLIPSE E300 Keywords 38

List of Figures

Figure 1 illustration of Scanning Curves generated from imbibition and drainage curves. 2
Figure 2 Projected 2D gas hysteresis process. 3
Figure 3 Water hysteresis model for increasing saturation (Christensen *et al.*, 2000) 3
Figure 4 – (a) Water relative permeability curve from an oil-water drainage experiment. (b) Gas relative permeability curves from an oil-gas experiment with connate water in it showing both imbibition (red) and drainage (blue). (c) Oil relative permeability including imbibition (red) and drainage in (blue) curves. (d) Oil relative permeability curve from an oil-gas and connate water drainage experiment. 4
Figure 5 5 modified SPE5 reservoir with grid dimension 35x35x50 (Model 1). 5
Figure 6 Anticline model with dipping angle of 6.5˚ (Model 2). 5
Figure 7 Heterogenous model with dimensions of 1067×1067×30 m with dipping angle of 6.5 degrees 6
Figure 8 shows oil saturations for a cross-section from 13to 23 in the J-direction after one year CO2-WAG injection. 7
Figure 9 CO_2 production rate (kg.mol/day) for (1) in red and (2) in blue. 7
Figure 10 Cross-sectional view of the Pressure Differential for line injection and inverted five spot patterns the pressure varies between 24 to 18 MPa. 8
Figure 11 CO_2 Saturation against time for 3,6 and 12 Months CO_2-WAG for non-hysteretic, WAG hysteresis simulation and WAG Hysteresis with CO_2 solubility. 9
Figure 12 shows the gas injection rate over time above and pressure over time below for soluble case (red) and CO_2 soluble. case in (blue). 10
Figure 13 Field Pressure for CO2 solubility in water (red) and without (blue). 10
Figure 14 shows the oil production rate (bbl/d). 10
Figure 16 Water-cut for the soluble cases shown in Fig. 15. 11
Figure 15 Cumulative oil produced after CO_2 separation with CO_2 solubility in water for different WAG ratios 11
Figure 17 CO_2-SWAG with CO_2 solubility in water displayed in red and without 11
Figure 18 Cumulative Oil Production for CO_2-SWAG (red) and three months CO_2-WAG (both models incorporate CO_2

solubility in water). Three month CO_2-WAG is compared against CO_2_SWAG and on the right hand plot the CO_2 production rate (m^3/day) is shown. 12
Figure 19 illustrates cumulative CO2 production separated from the oil stream. 12
Figure 20 illustrates a comparison of CO_2 dissolved in the aquous phase after 20 years of EOR for CO_2-WAG and CO_2-SWAG injection. 13
Figure 21 comparison of CO_2 production rate (kg.mol/day) for box model (Model 1) and dipping model (Model 2). 13
Figure 22 Cumulative oil produced over 20 years of EOR for CO2-SWAG (red) and CO2-WAG (blue). 14
Figure 23 Cross-sectional view of oil saturation for model 2 after two years of EOR 14
Figure 24 Final oil saturation distribution of SWAG and CO2-WAG after 20 years of EOR 14
Figure 25 Phase Diagram at bottom hole pressure constraint of 17.2 MPa at reservoir temperature of 71 degrees Celsius 36
Figure 26 Ternary plot of Fluid at 17.2 MPa with reservoir temperature at 71 C 36
Figure 27 Slimtube Simulation to determine the Minimum Miscibility Pressure (MMP) of the compositional Fluid model 36
Figure 28 Heterogenous Model using Model 2 with varying porosity and permeability distribution 37

MSc in Petroleum Engineering 2013-2014

Imperial College London

Carbon Dioxide Enhanced Oil Recovery

Abdul Rafay Zafar

Professor Martin J. Blunt, Imperial College London

Marie Ann Giddins, Schlumberger

Abstract

This paper examines the use of compositional fluid models for miscible CO_2 injection studies. We analyzed the effects of CO_2 solubility effects for miscible CO_2-WAG and CO_2-SWAG EOR strategies. The simulations were performed in a homogenous and a more complex heterogeneous sector model. For this study we used a synthetic realistic three-phase permeability model using Oak's three-phase relative permeability curve end points (Oak, 1991) and to demonstrate three-phase WAG hysteresis we used the Larsen and Skauge (1998) model. This paper concludes by discussing the effects of CO_2 solubility in CO_2 water alternating gas injection (WAG) and simultaneous water alternating gas injection (SWAG). We demonstrated the significance of including CO_2 solubility in water to quantify potential CO_2 injectivity losses in CO_2 –WAG strategies. We also demonstrate advantages of implementing CO_2 – SWAG injection in heterogeneous reservoir to maximize oil recovery. Depending on the project objective (1) maximizing oil recovery we recommend CO_2-SWAG injection (2) CO_2-EOR and sequestration CO_2-WAG is recommended. For CO_2-WAG simulations we propose to incorporate three-phase relative permeability hysteresis effects in conjunction with CO_2 solubility effects in water.

Introduction

Carbon dioxide enhanced oil recovery in depleted oil reservoirs has been employed since the 1970s. Depleted oil reservoirs are known locations for previously trapped hydrocarbons for long periods and can be safely regarded as a sealed destination for CO_2 sequestration purposes. The ultimate goal of a CO2-EOR project is the ability to extract additional reserves by utilizing the advantageous properties of CO_2, such as high solubility in oil and significant reduction in oil viscosity, which improves the mobility of crude oil in the formation. A great emphasis is placed for miscible CO_2-flooding, which depends on the minimum miscibility pressure of the fluid in place (Lake, 1989, Dake, 1979).

For the past three decades extensive research has been conducted to study the effects of three-phase relative permeability changes in WAG process. Several empirical methods have been developed to honor the petro-physical behavior of certain rock types. Rock structure, wettability and fluid type affect the multi-phase flow through the porous medium (Blunt *et al.*, (2012)). Land's trapping parameter is a necessary input for Killough's hysteresis model to account for the trapping of the non-wetting phase. The model is based on the saturation history of the reservoir where Killough (1976) demonstrated water hysteresis using an interpolation method with water relative permeability curves, which are bounded between imbibition and drainage curves. When the trapping coefficient is small, a higher trapped gas occurs during an imbibition process, hence an increase in oil recovery and sweep efficiency is obtained (Spiteri *et al.*, (2004)). Several studies stated that gas trapping effects and can only be account if a valid hysteresis model is considered (Blunt, 2000; Kossack, 2000; Spiteri *et al.* (2008).

A common issue associated with CO_2-WAG projects is injectivity losses resulting in decreased injection pressure cycles. The injectivity of water is influenced by the trapped gas saturation, which affects the available miscible gas to mix with the oil and lowers the total mobility of the system (Rogers et *al.*, (2001). Krumhansel *et al.* (2002) simulated the effectiveness of CO_2 sequestration in depleted reservoirs and showed that small quantities of CO_2 dissolve in water. Ennis-King *et al.* (2005) demonstrated that convective mixing is of great importance for CO_2 dissolution in water during a CO_2 injection phase with the emphasis that in reality the dissolution happens in a shorter time frame than expected. Pollack et al. (1988) conducted a study of CO_2 and hydrocarbon systems with presence of an aqueous phase. Their findings showed that the presence of water in the system reduces the amount of CO_2 accessible for mixing with *in-situ* hydrocarbons.

According to Qi et al (2008) simultaneous water alternating gas (SWAG) injection has a better mobility contrast compared to the traditional WAG injection. The CO_2 sweeps the top part and water displaces oil in the bottom part of the reservoir. SWAG injecting achieves more favourable sweep efficiency and better oil recovery.

In this study a synthetic reservoir model is used to investigate CO_2 injection strategies and the impact of hysteresis in CO_2 WAG floods. The significance of CO_2 solubility in water is demonstrated for CO_2 –WAG and CO_2 –SWAG EOR strategies.

Relative Permeability Hysteresis

In CO_2-WAG process three phases flow simultaneously under sequential changes between CO_2 injection and waterflooding. There are distinct differences between drainage and imbibition models. Spiteri *et al.* (2004) defined hysteresis as "irreversibility" or "path dependence". During drainage process a monotonic decrease of the wetting saturation takes place. During an imbibition process there is a monotonic increase of the wetting phase see **Fig. 1**.

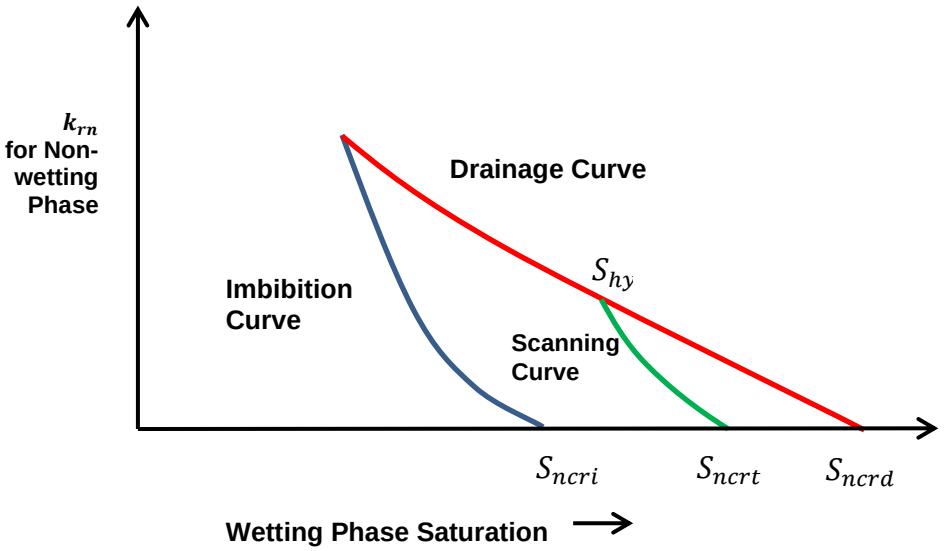

Figure 1 illustration of Scanning Curves generated from imbibition and drainage curves.

Land trapping model

The trapping of the non-wetting phase after flow reversal is the most influential factor defining the consequences of hysteresis effects. Land's trapping model is the foundation for numerous hysteresis models. Land's trapping parameter (C) varies with fluid type and permeability. It is important to note that large values of C a low trapping of the non-wetting phase is predicted. To validate the trapping parameter scanning curves with varying gas saturations at flow reversal $(S_{g,hy})$ have to be compared with the laboratory and simulated results (Land, 1942). In Land's trapping model the trapped gas saturation is defined as

$$S_g = S_{gf} + S_{gr} \quad \text{.....(1)}$$

Land's trapping coefficient is defined as

$$C = \frac{1}{S_{gr}} - \frac{1}{S_{gi}} \quad \text{.....(2)}$$

$$S_{g,trap} = S_{g_{cr}} + \frac{(S_{g_m} - S_{g_{cr}})}{1 + C\,(S_{g_m} - S_{g_{cr}})} \quad \text{.....(3)}$$

In a gas-oil experiment the gas relative permeability (k_{rg}) is defined as

$$k_{rg}(S_g) = k_{rg}^{d}\,(S_{gf}) \quad \text{.....(4)}$$

where

$$S_{gf} = S_{g_{cr}} + \frac{1}{2}\left[\left(S_g - S_{g_{trap}}\right) + \sqrt{\left(S_g - S_{g_{trap}}\right)^2 + \frac{4}{C}\left(S_g - S_{g_{trap}}\right)}\ \right] \quad \text{.....(5)}$$

Larsen and Skauge Three-Phase Hysteresis model

Larsen and Skauge (1998) extended Killough models by formulating a hysteresis model for both wetting and non-wetting phase, which takes into account cyclic relative permeability changes during WAG injection. As a result, the trapped gas saturation becomes history dependent. In this model the secondary imbibition and drainage curves are not parallel to the primary relative permeability curves. In **Fig. 2** an illustration is provided for the drainage and imbibition process a gas phase. During a drainage process the gas relative permeability follows the primary drainage curve. In an imbibition process the primary is not traced anymore and follows a path parallel to the primary drainage curve. A damping factor is introduced for the increasing gas relative permeability, which is determines the start of the secondary drainage curve.

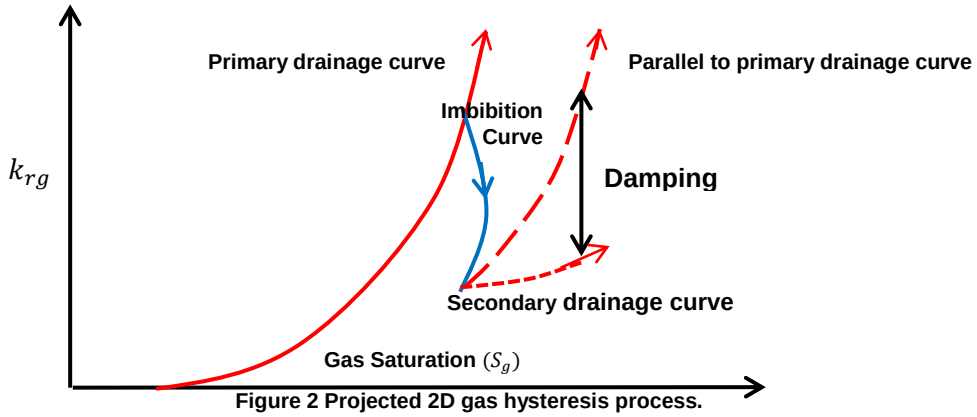

Figure 2 Projected 2D gas hysteresis process.

The drainage gas relative permeability is defined as

$$k_{rg}^{drain} = \left[k_{krg}^{input} - k_{krg}^{input}\left(S_g^{start}\right) \cdot \left[\frac{S_{wc}}{S_w^{start}}\right]^{\alpha} + \left(k_{rg}^{imb}\left(S_g^{start}\right)\right)\right] \quad \text{.....(6)}$$

During cyclic gas injections a reduction in gas relative permeability will occur under the conditions of cyclic water injection water saturation tends to increase. During an imbibition process the drainage curve is defined by

$$k_{rg}^{imb,n}\left(S_g\right) = k_{rg}^{drain,n}\left(S_{gf}^{trans}\right) \quad \text{.....(7)}$$

where n is the number of hysteresis cycles

$$S_{gf} = S_{g_{cr}} + \frac{1}{2}\left[\left(S_g - S_{g_{trap}}\right) + \sqrt{\left(S_g - S_{g_{trap}}\right)^2 + \frac{4}{C}\left(S_g - S_{g_{trap}}\right)}\ \right] \quad \text{.....(8)}$$

For an imbibition process for a wetting phase the water saturation increases and the water relative permeability is interpolated between two-and three-phase curves, which are dependent on the trapped gas saturation, which is illustrated in **Fig. 3**

$$k_{rw}^{imb} = k_{rw_2}\left(1 - \frac{S_g^{start}}{S_{g,max}}\right) + k_{rw_3}\left(\frac{S_g^{start}}{S_{g,max}}\right) \quad \text{.....(9)}$$

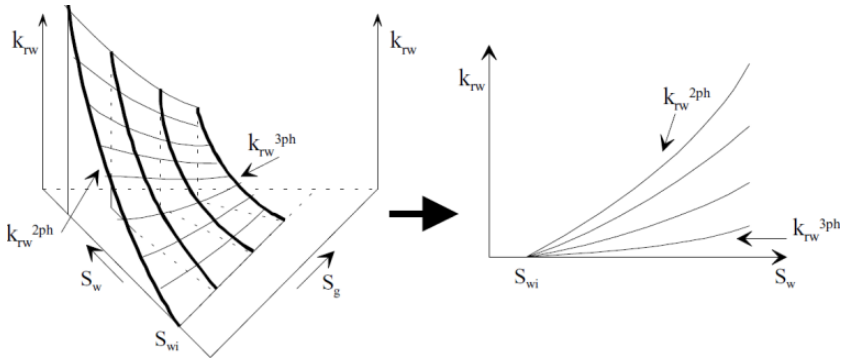

Figure 3 Water hysteresis model for increasing saturation (Christensen *et al.*, 2000)

Methodology

Relative Permeability Curves

For this study, a synthetic relative permeability model was developed, to illustrate the effects of three-phase WAG Hysteresis. We used the end-points of the three-phase relative permeability data from Oak (1991) from the oil-water and gas-oil experiment in **Fig. 4** below. In Oak's experiment Land's coefficient varies between 0.7 and 2.2 (Spiteri and Juanes, 2004). In this study we used a trapping coefficient of $C = 2$, a damping coefficient α =1.0.

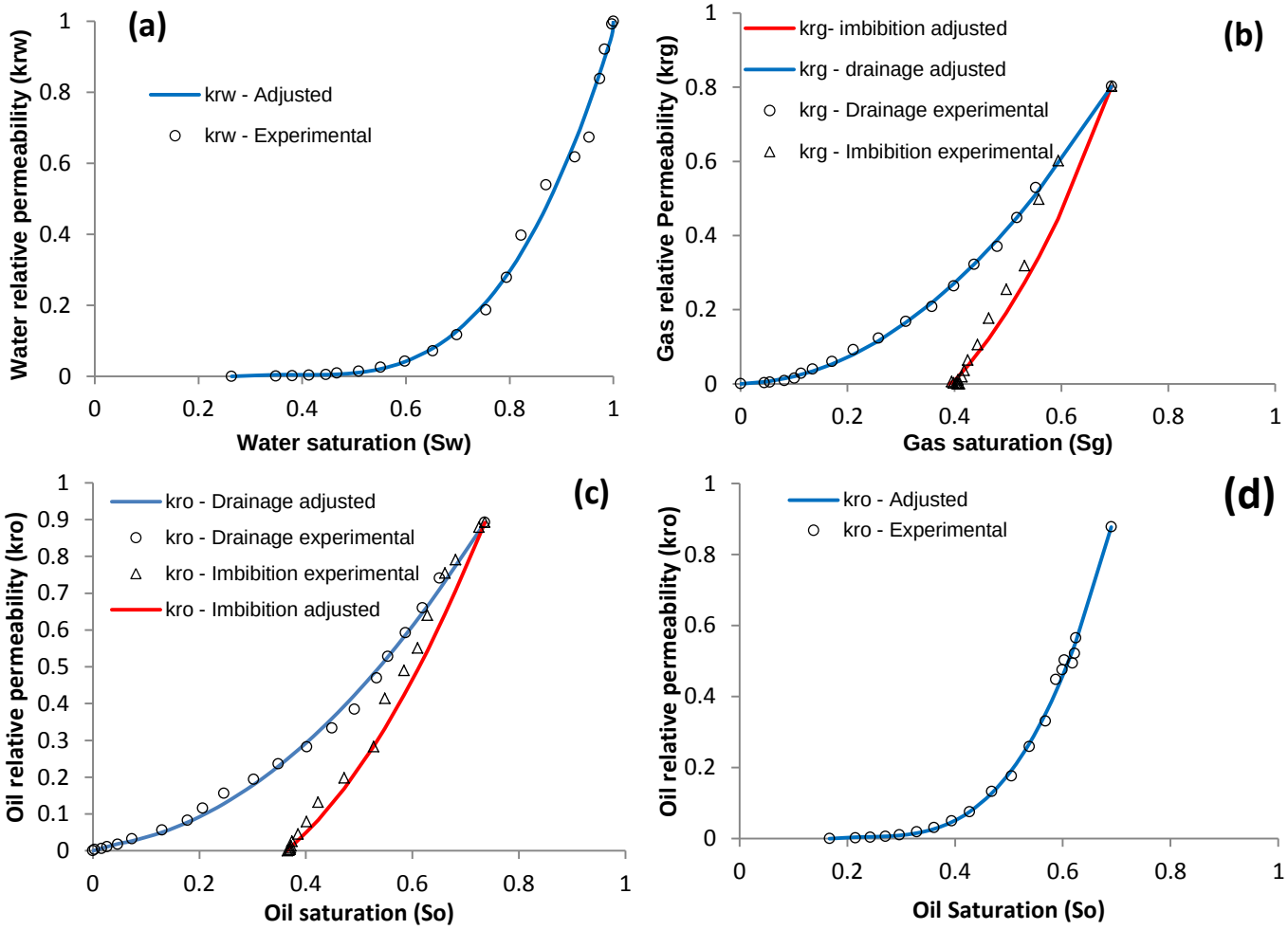

Figure 4 – (a) Water relative permeability curve from an oil-water drainage experiment. (b) Gas relative permeability curves from an oil-gas experiment with connate water in it showing both imbibition (red) and drainage (blue). (c) Oil relative permeability including imbibition (red) and drainage in (blue) curves. (d) Oil relative permeability curve from an oil-gas and connate water drainage

Fluid Model

For the purpose of this study we modified the volatile oil Equation of State model from the fifth comparative solution paper (Killough and Kossack, 1987) to include a CO_2 component. **Table 1** shows the initial reservoir oil composition. The bubble point pressure is 15.9 MPa (2300 psi). A Slimtube simulation was performed to determine the Minimum Miscibility Pressure (MMP), which was determined at 16.5 MPa (2386 psi). According to the EOS estimations the MMP is 16 MPa (2323 psi).

Component	*Mole fraction*
CO2	0
C1	0.5
C3	0.03
C6	0.07
C10	0.2
C15	0.15
C20	0.05

Table 1 Modified Fluid model from the fifth comparative solution paper (SPE 16000)

Homogenous model description

For our analysis we modified the homogenous water-wet SPE5 model (Killough and Kossack, 1987). The reservoir dimension is 1067 m in x and y direction with reservoir thickness of 30 m and is fully oil saturated. The original SPE5 grid dimension is 7×7×3. The reservoir lithology is considered as Sandstone with a uniform porosity of 0.3. The initial reservoir pressure is 27.6 MPa and the reservoir temperature is 71 degrees Celsius. A summary of the reservoir properties is provided in **Table 2.** For this study for a refined grid with dimensions 35×35×50 was used to reduce numerical dispersion effects of composition (**Fig. 5 & 6**). The stock tank oil in place (STOIIP) is 43 million m^3 and a reservoir pore volume of 0.43.

Reservoir Layer	Thickness	k_{xy}	k_z	kv/kh Ratio
Layer 1	6 m	500md	50md	0.10
Layer 2	9 m	50md	50md	1
Layer 3	15 m	200md	25md	0.13

Table 2 Reservoir properties for homogenous grid models.

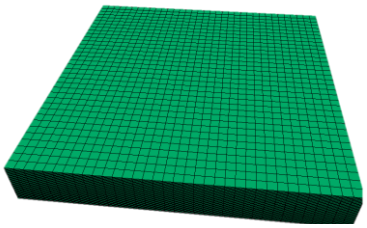

Figure 5 5 modified SPE5 reservoir with grid dimension 35x35x50 (Model 1).

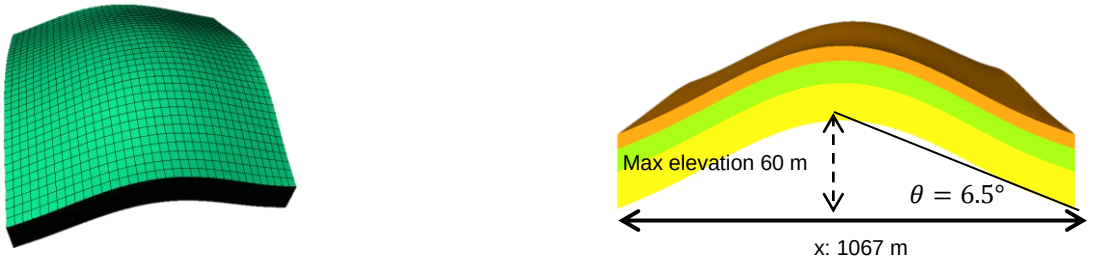

Figure 6 Anticline model with dipping angle of 6.5˚ (Model 2).

Injection Strategy and Pattern

CO_2-WAG

We investigated two strategies in order to isolate physical effects; (1) one injector and one producer is positioned in each corner. (2) Inverted five spot pattern was implemented four injectors and one producer. Before implementing an EOR strategy the reservoir is naturally depleted for 90 days followed by two years of waterflooding. Simulations were analyzed for 3, 6 and 12 months CO_2-WAG cycles for 20 years, which is equivalent to inject 1.2 pore volumes (PV) of injection fluids. The injection is also controlled by voidage replacement of 1. **Table 3** illustrates the target rates and constraints for each well for the two injection pattern. In our study we also investigated different WAG ratios where the CO_2 Slug size was varied for short and long injection periods, which is presented in **Table 4**. We conducted our analysis by using Larsen & Saige WAG Hysteresis model and non-hysteretic simulations.

	(1) corner-to-corner	(2) inverted 5Spot
Oil production rate (m^3/day)	1272	1272
Production BHP (MPa)	17.2	17.2
Water injection rate (m3/day)	1272	318
Gas injection rate (10^6 m^3/day)	467	116.8
Injector BHP (MPa)	6.9	6.9

Table 3 Summary of producer and injector target rates with BHP constraints

	CO_2 injection	Water Injection
WAG Ratio 1:2	3 Months	6 Months
	6 Months	12 Months
	12 Months	24 Months
WAG Ratio 2:1	6 Months	3 Months
	12 Months	6 Months
	24 Months	12 Months

Table 4 Summary of CO_2-WAG ratio

CO_2-SWAG

Similar to the CO_2- WAG injection strategy in the CO_2-SWAG the reservoir is naturally depleted for 90 days followed by two years of waterflooding then CO_2-SWAG is implemented for 20 years. The rates have been adjusted accordingly to match the same injection volumes of the CO_2-WAG strategy. In this strategy gas and water are injected simultaneously with gas injected in the top perforations and water in the bottom perforations of the injection wells. A summary of the CO_2-SWAG can be found in **Table 5.**

	(1) corner-to-corner	**(2) inverted 5 Spot**
Oil production rate (m^3/day)	1272	1272
Production BHP (MPa)	17.2	17.2
Water injection rate (m^3/day)	328	82
Gas injection rate (Mm^3/day)	159	39.6
Injector BHP (MPa)	6.9	6.9

Table 5 Production and injection target rates for CO_2-SWAG

Heterogeneous model description

After conducting the homogenous simulations we apply the techniques on a heterogeneous sector model, with a dipping angle of 6.5 degrees (**Fig. 7**). A summary of the reservoir properties is shown in **Table 6**. For the injection strategy the reservoir is naturally depleted for 90 days followed by two years of waterflooding. The oil production rate is 477 m^3/day with BHP limit of 17.2 MPa. After the natural depletion water is injected for 80 m^3/day with BHP limit of 6.9 MPa. In the *CO_2-WAG* gas is injected with a rate of 28 million m^3/day and water injection is kept at the same rate. During CO_2-WAG the injectors BHP is kept at 6.9 MPa. On the other hand, for *CO_2-SWAG* gas and water are injected simultaneously with rates 10 million m^3/day and 3.2 m^3/day, respectively. In both EOR strategies the inverted five spot pattern was simulated for 20 years.

STOIIP	27 million m^3
Reservoir pore volume	0.34
average horizontal permeability	233 mD
average vertical permeability	28 mD
average porosity	0.15
Producers (P)/Injectors (I)	1P/4I
Well pattern	inverted five spot pattern
Producer well spacing	1000 m
Water-cut prior to CO_2-EOR	-

Table 6 Summary of heterogenous properties.

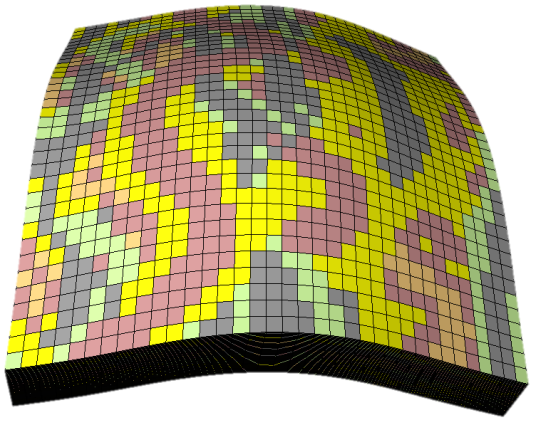

Figure 7 Heterogenous model with dimensions of 1067×1067×30 m with dipping angle of 6.5 degrees

Results and Analysis

Grid sensitivity study for compositional simulations

A miscible CO_2-WAG grid sensitivity was conducted for discretized cells ranging from 0.35-3.5 m in vertical thickness and a horizontal length of 30.5 m, which represented the SPE 5 model with dimensions 1067×1067×35 m. The horizontal length of 30.5 m was recommended according to Sifuentes *et al.* (2007). In **Fig. 8** a cross-sectional oil saturation profile is shown. Comparing the gridblock dimensions with vertical thickness of 1.5 and 3.5 m against the finest layering of 0.35 m vertical thickness it can be observed that the numerical dispersion effects are significant. However, the difference between 0.35 m and 0.70 m vertical layering is minor. For the purpose of our study, we selected a vertical layering of 0.70 m.

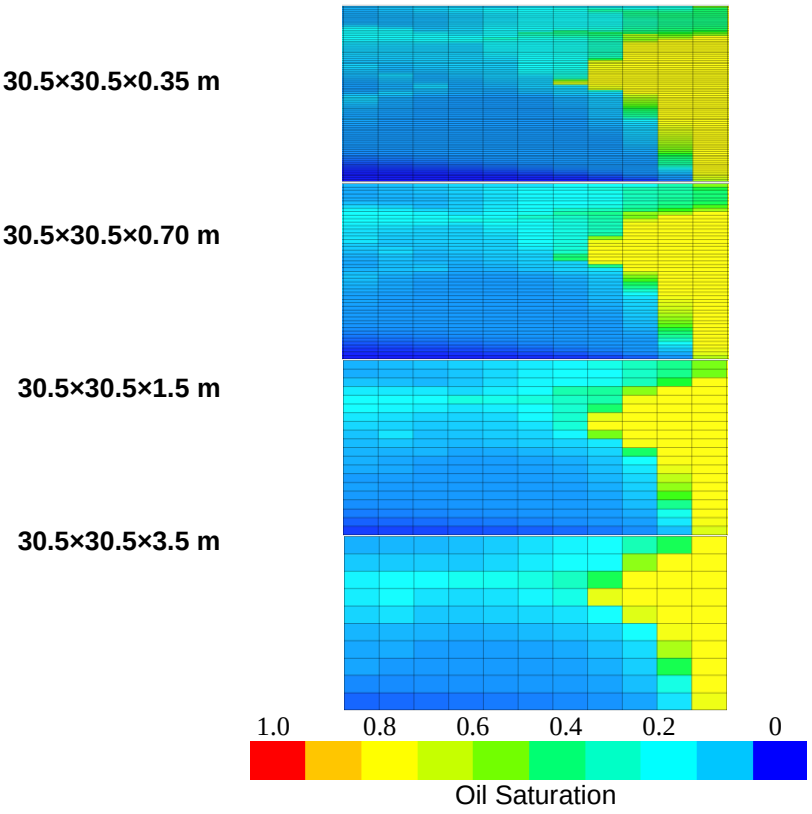

Figure 8 shows oil saturations for a cross-section from 13to 23 in the J-direction after one year CO2-WAG injection.

Effectiveness of injection patterns

We begin by showing the differences of the injection patterns, which influences the CO_2 plume movement through the formation in the box model; (1) line injection and (2) inverted five spot pattern. We inject the same quantity of CO_2 and water for both patterns for 20 years. In **Fig. 8** the CO_2 production rate (m^3/day) for a six months CO_2- WAG cycle is shown for the line-drive and inverted five spot pattern. CO_2 is produced later in the line-drive, but more CO_2 is produced towards the end of the production period.. The injection pressure from the single well in the line drive model is much higher than for injection wells in the five spot pattern because of the higher injection volume. In **Fig. 9** the field pressure is shown for a six months CO_2 –WAG.

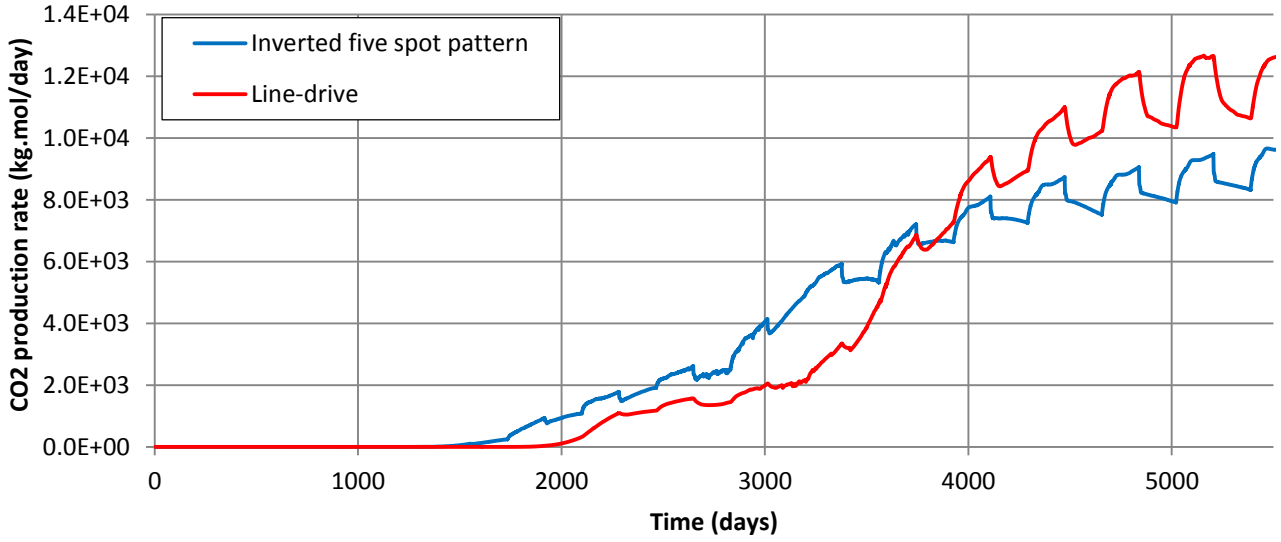

Figure 9 CO_2 production rate (kg.mol/day) for (1) in red and (2) in blue.

In **Fig. 10** the pressure distribution is shown for both patterns. The pressure difference between injector and producer in the line drive model is higher compared to the inverted five spot pattern. Therefore in the line-drive pattern the CO_2 plume travels faster in the formation.

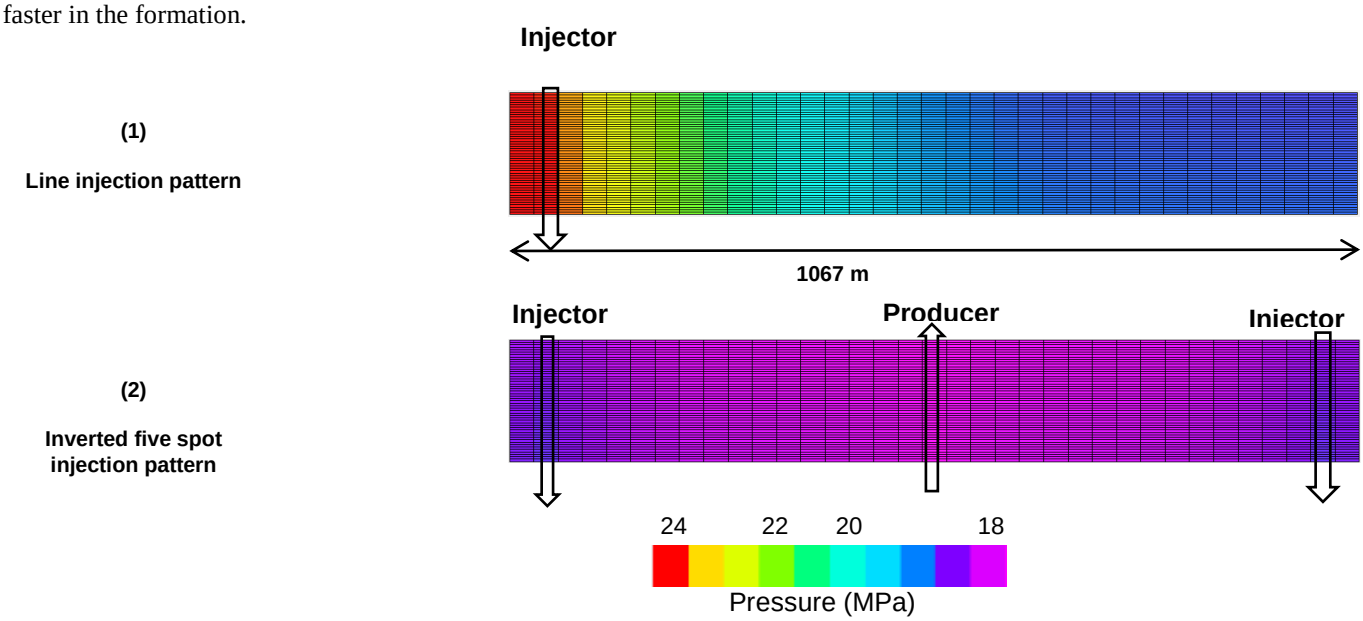

Figure 10 Cross-sectional view of the pressure differential for line injection and inverted five spot patterns the pressure varies between 24 to 18 MPa.

Small scale CO_2 solubility and trapping effects

We compare the following models: non-hysteretic, Larsen & Skauge WAG hysteresis model, Larsen &Skauge WAG hysteresis model with CO_2 solubility in water for in block (16, 5, 1) and (17, 18, 10) for the WAG intervals three months, six months and one year. Block (16, 5, 1) is near the top surface and block (17, 18, 10) is in the centre of the formation. In **Fig. 11** the block gas saturation of (16, 5, 1) and (17, 18, 10) on the left hand and right hand sight, respectively.

3 Months CO_2-WAG. In block (16, 5, 1) more CO_2 trapping occurs in the hysteresis models. Also more CO_2 is trapped after each water injection cycle. In block (17, 18, 10) no decrease in gas saturation is observed, because of continuous gas flow.

6 Months CO_2-WAG. In block (16, 5, 1) the gas saturation decreases significantly after each water injection cycle. More CO_2 is trapped after each water flood in the solubility model. In block (17, 18, 10) the gas saturation behaviour is similar to the *3 Months CO_2-WAG* simulation but a delayed gas increase is observed, because of decreased CO_2 injectivity.

12 Months CO_2-WAG. Less CO_2 trapping is observed in (16, 5, 1) after each water flood. In block (17, 18, 10) cyclic variation in CO_2 saturation is observed. A more significant delay in CO_2 saturation increase is observed for the CO_2 solubility model.

Small scale CO_2 trapping effects are sensitive to the CO_2 injection period. Short CO_2 injection cycles result in lower decrease in CO_2 saturation in the top layer of the reservoir. The loss in CO_2 injectivity will be discussed in the next section when analyzing the macroscopic CO_2 solubility effects.

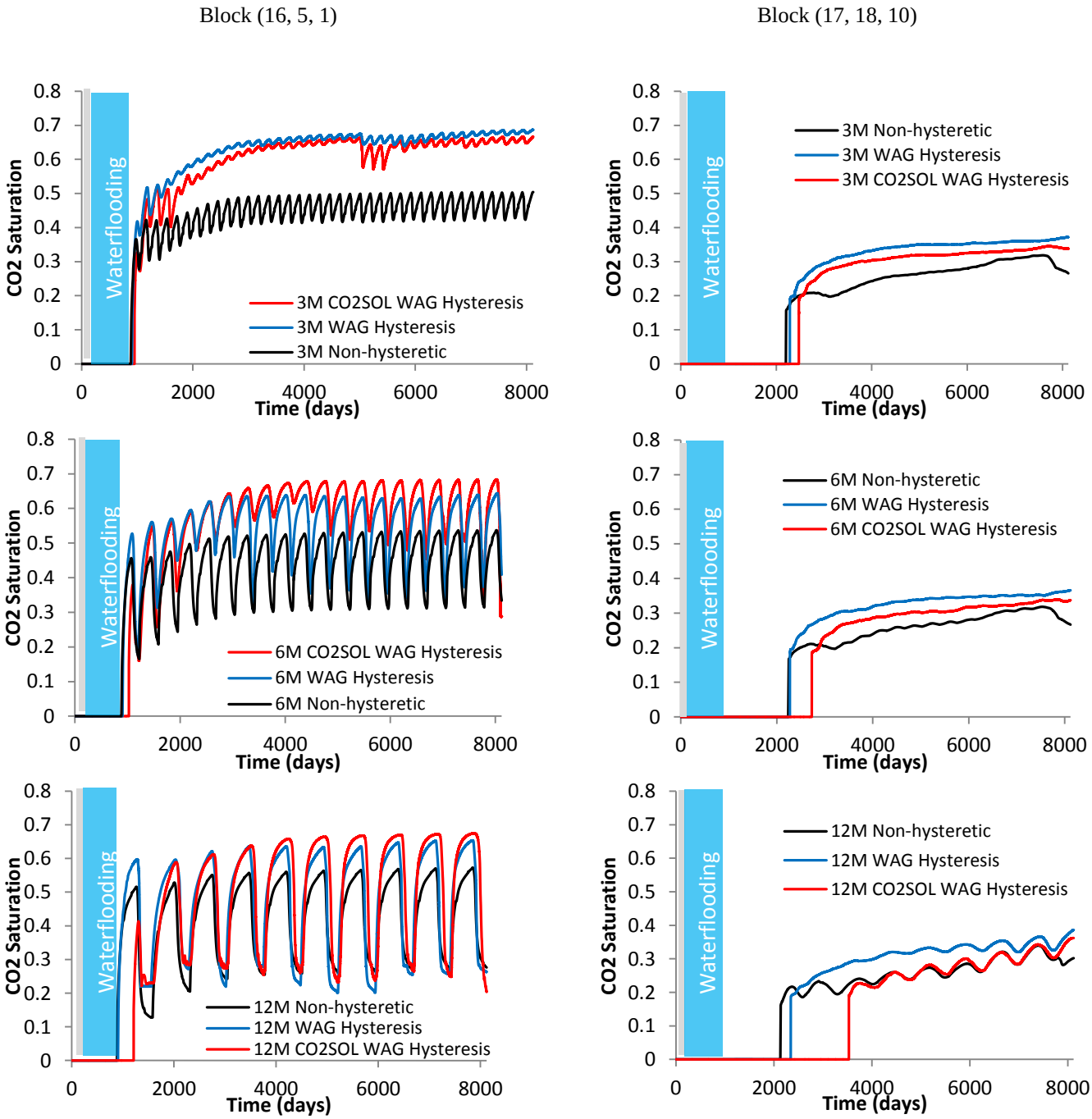

Figure 11 CO_2 Saturation against time for 3,6 and 12 Months CO_2-WAG for non-hysteretic, WAG hysteresis simulation and WAG hysteresis with CO_2 solubility.

Macroscopic effects of CO_2 solubility

In this section we show the results of CO_2 solubility in water displayed in (red) and without (blue). Both models incorporate Larsen & Skauge hysteresis model. **Fig. 12** illustrates gas injection (m^3) over time, immediately after the waterflooding period for two a significant loss in gas injection is observed when CO_2 solubility is considered.

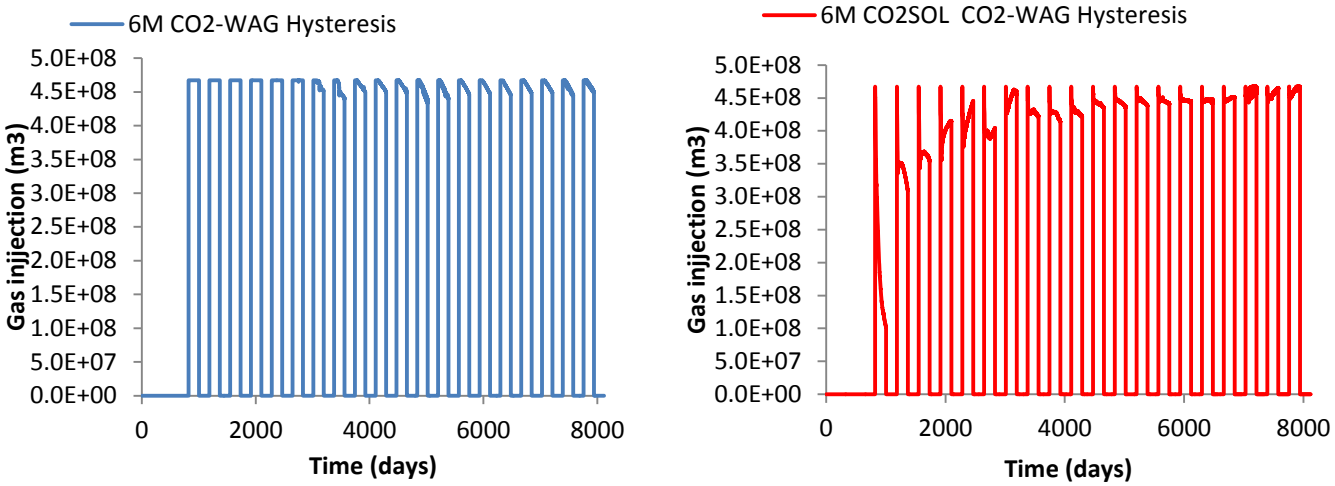

Figure 12 shows the gas injection rate over time above and pressure over time below for soluble case (red) and CO_2 soluble.

In **Fig. 10** Pressure (MPa) over time is shown. For the simulation with CO_2 solubility a sharp pressure decrease occurs after every gas injection cycle. In **Fig. 13** a similar decrease in oil production rate is observed for the CO_2 solubility case. The decrease in oil production occurs after implementing CO_2 injection. The oil production increases from 200 m^3/day to 700 m^3/day after four CO_2-WAG cycles.

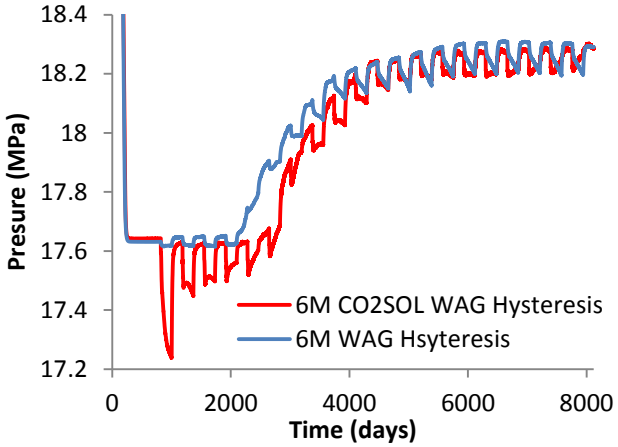

Figure 13 Field Pressure for CO_2 solubility in water (red) and without (blue).

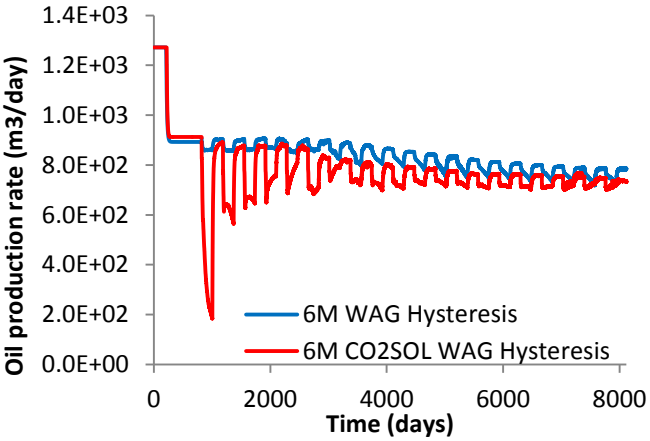

Figure 14 shows the oil production rate (bbl/d).

As shown in **Fig. 11** the reduced injection volumes due to CO_2 solubility in water mean that the CO_2 trapping effect is delayed.

Impact of CO_2 solubility for different WAG Ratio

We now investigate the effectiveness of varying CO_2 WAG ratios. We have taken into account Larsen and Skauge hysteresis model and the solubility of CO_2 in water. In **Fig. 15** cumulative oil is presented after CO_2 separation for two different WAG cycles (three months gas followed by 6 months water; and 6 months gas followed by 12 months water). The longer cycle results in slightly higher cumulative oil production. In **Fig. 16** water-cut of the CO_2 soluble cases is presented. For both cases the water-cut commences after 2000 days but a higher water production is observed for the three months CO_2 injection and six months waterflooding. However, after 4000 days there is a significant increase in water-cut for the six months CO2 injection and one year waterflooding.

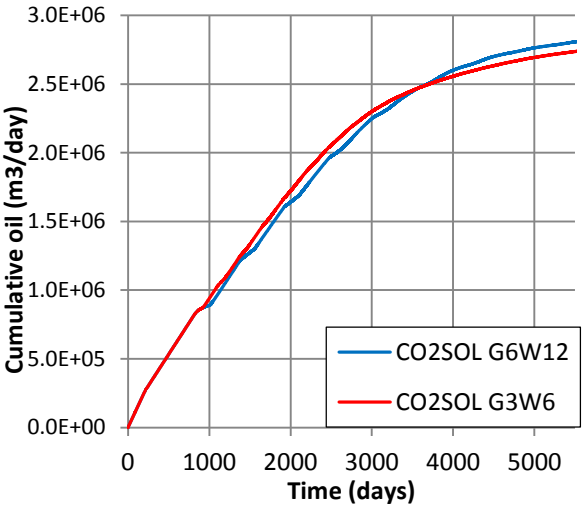

Figure 16 Cumulative oil produced after CO_2 separation with CO_2 solubility in water for different WAG ratios

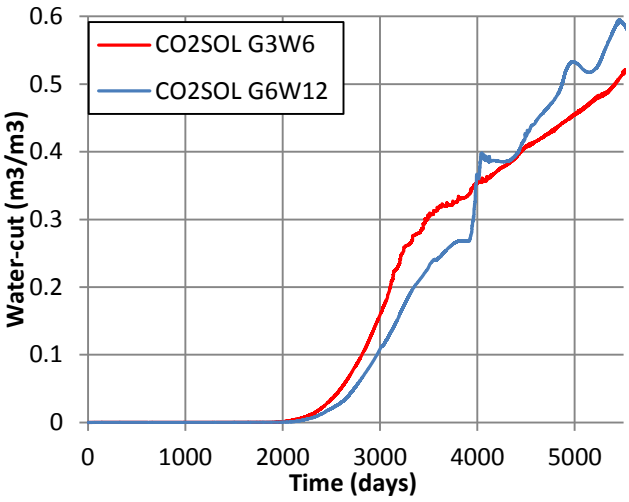

Figure 15 Water-cut for the soluble cases shown in Fig. 15.

CO_2 –SWAG injection

Fig. 17 shows the cumulative oil produced after CO_2 separation for CO_2-SWAG with CO_2 solubility in water (red) and without (blue). There is a small increase in total production for the case with CO_2 solubility.

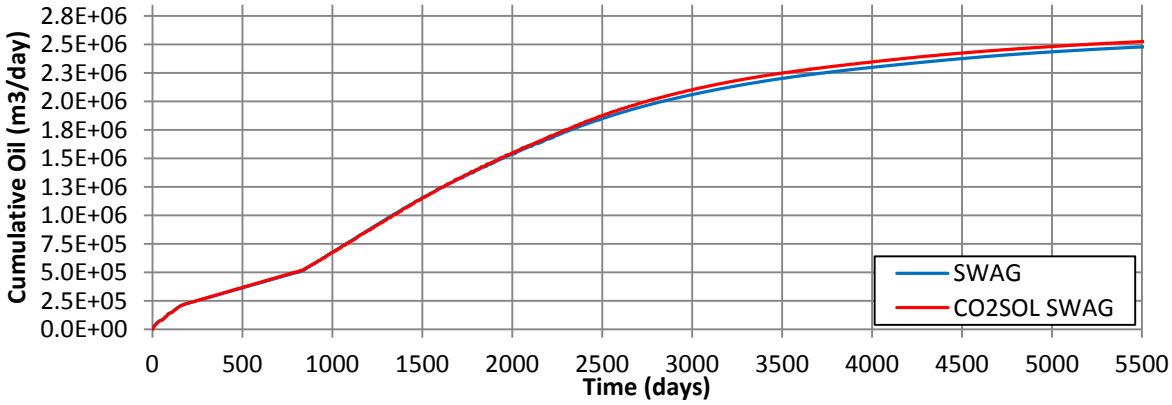

Figure 17 CO_2-SWAG with CO_2 solubility in water displayed in red and without

However, in **Fig.18** cumulative oil production is shown for CO_2-SWAG and three months CO_2-WAG. Both simulation results include CO_2 solubility in water. After 3500 days CO_2-SWAG recovers more oil than CO_2-WAG strategy. On the right hand CO2 production for six months CO_2 injection and one year waterflooding against the SWAG case is presented. From this plot it can be identified that SWAG is more favourable in the long-term, because of decreased CO_2 production. For CO_2-WAG the production of CO_2 remains constant in the long-term.

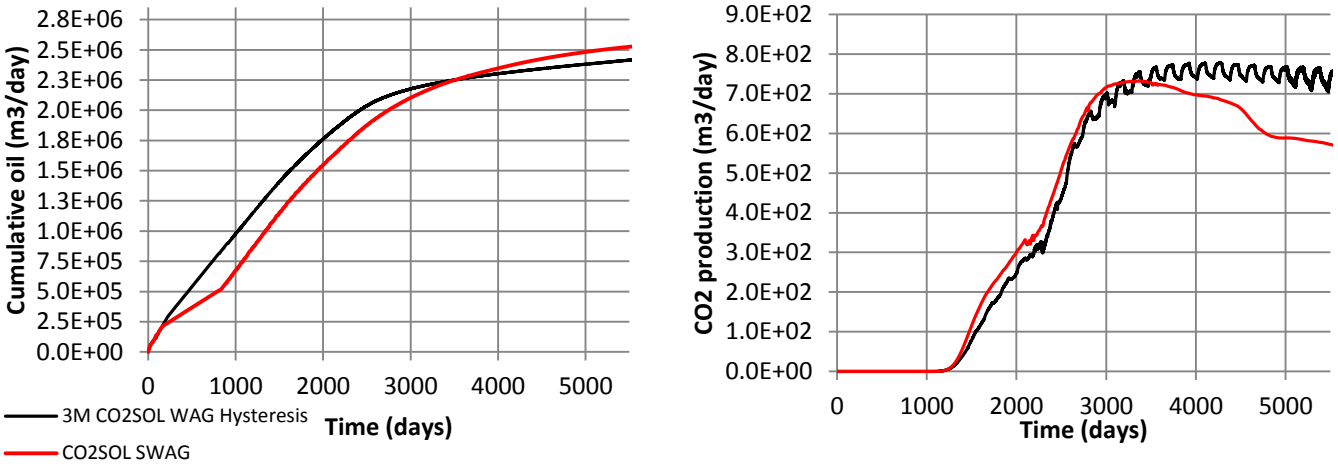

Figure 18 Cumulative Oil Production for CO_2-SWAG (red) and three months CO_2-WAG (both models incorporate CO_2 solubility in water). Three month CO_2-WAG is compared against CO_2_SWAG and on the right hand plot the CO_2 production rate (m^3/day) is shown.

In **Fig. 19** the cumulative oil produced is compared for a WAG ratio of 1:2 against SWAG injection strategy under similar injection volumes for CO_2 and water. For the SWAG simulation very early gas breakthrough and high water-cut occurred, because of the homogenous distribution of the reservoir. Both CO_2 and water separate after simultaneous injection, because of the lower density of CO_2. The CO_2 plume dissolves the oil at the top structure of the reservoir and follows a continuous path through the top layers.

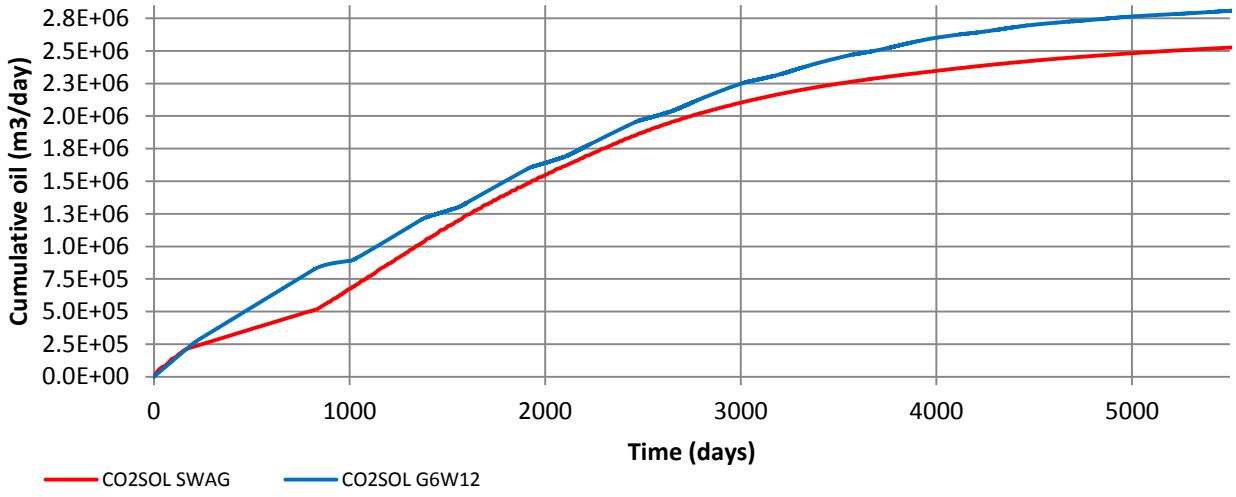

Figure 19 illustrates cumulative CO_2 production separated from the oil stream.

Coupled CO_2-EOR and CO_2 sequestration

In this section we investigate the effectiveness of CO_2 sequestration for CO_2-WAG and CO_2-SWAG in a homogenous model with dipping angle. In **Fig. 20** the dissolution of CO_2 in water after 20 years of EOR is shown. In the CO_2 –WAG strategy of six months gas injection and one year waterflooding 203761 tonnes of CO_2 is dissolved in the reservoir. For CO_2 –SWAG 122156 tonnes of CO_2 is dissolved in the reservoir.

CO_2-WAG: after the waterflooding period the CO_2 plume dissolves in the aqueous phase. In this model gravity effects contribute with the CO_2 mixing. A significant amount of water accumulates near the injection wells. Less CO_2 is dissolved in top structure, because of a continuous flow path.

CO_2-SWAG: little CO_2 is dissolved in the bottom of the formation, because the perforations for gas injection are in the top half and water is injected in the bottom half of the injector. More CO_2 is accumulated near the injection site, because of gravity effects.

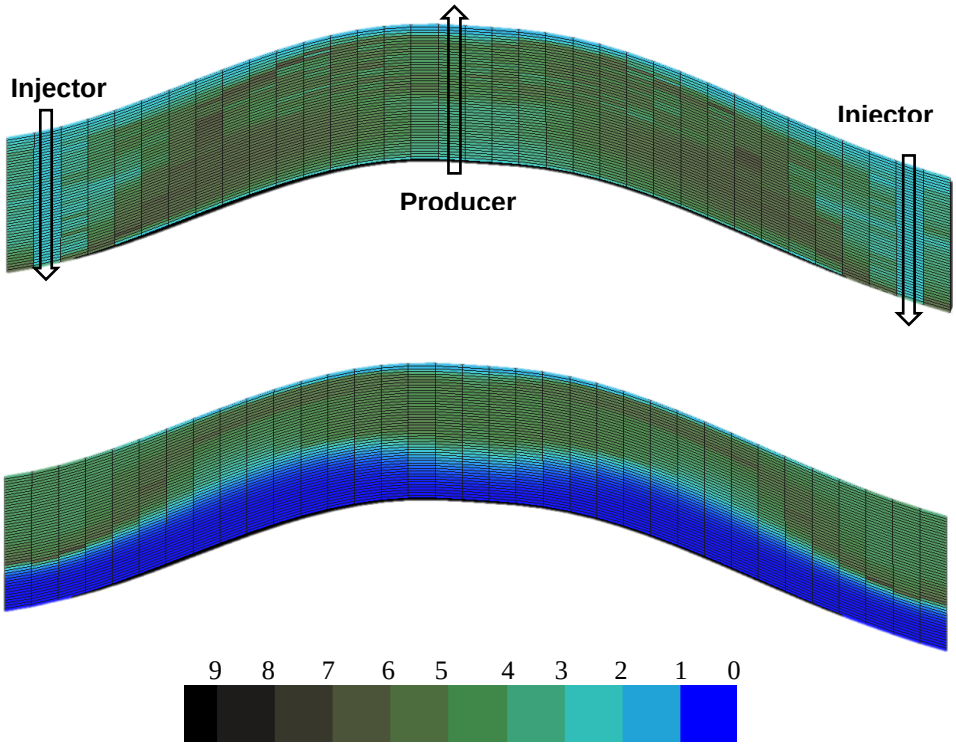

Figure 20 illustrates a comparison of CO_2 dissolved in the aquous phase after 20 years of EOR for CO_2-WAG and CO_2-SWAG injection.

In this homogenous dipping model gravity override is more severe. The effectiveness of simultaneous gas and water injection to displace the oil is significantly reduced. The CO_2 breaks through more rapidly in the CO_2-SWAG compared to the homogenous box model (Model 1) see **Fig. 21**.

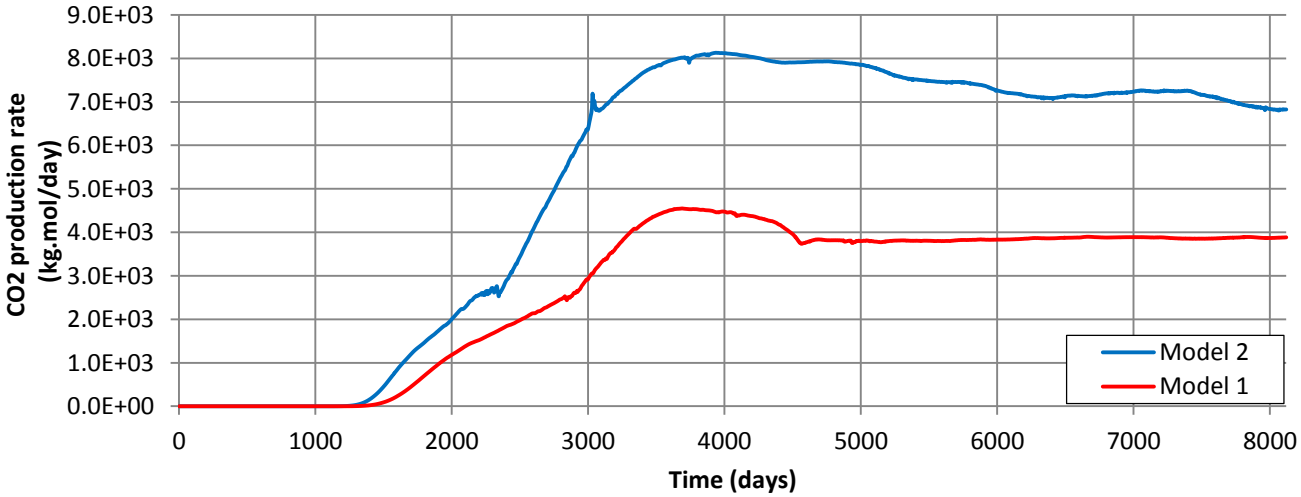

Figure 21 comparison of CO_2 production rate (kg.mol/day) for box model (Model 1) and dipping model (Model 2).

Heterogeneous application

In the heterogeneous model the top layer consists of low permeability and porosity distributions (see Appendix: Heterogeneous model). The middle layers have higher permeability and the lower layers have medium permeability.After implementing the EOR strategy SWAG obtained higher cumulative oil (**Fig. 22**). In the CO_2-SWAG simulation the CO_2 travels through the high permeability channels in the middle layer first creating a continuous flow path to the injector. Similar to the homogenous models a higher CO_2 production and water-cut is observed for SWAG. **Fig. 23** shows a cross-sectional view of the oil saturation after 2 years of EOR and an areal view of the final oil saturation is presented in **Fig. 24**. The CO_2-SWAG strategy in the heterogeneous reservoir achieved lower final oil saturation. Moreover, a better mobility contrast and sweep efficiency was obtained, compared to the CO_2-WAG strategy. The injected fluid travels faster in the SWAG simulation and is able to sweep the top structure of the reservoir, which has a lower horizontal and vertical permeability. In this model viscous fingering and gravity effects can be observed for both strategies. Those effects are more significant in the CO_2 – WAG strategy and more oil has been bypassed.

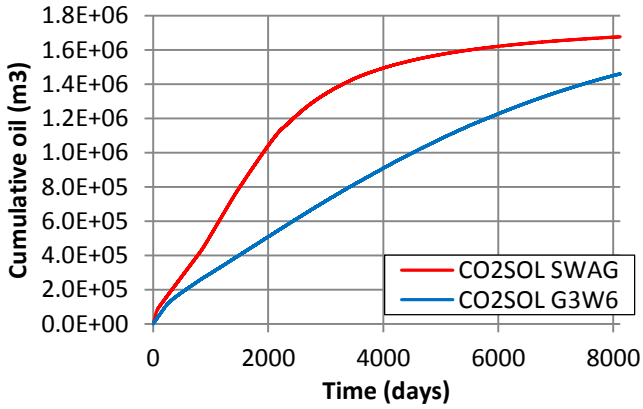

Figure 22 Cumulative oil produced over 20 years of EOR for CO2-SWAG (red) and CO2-WAG (blue).

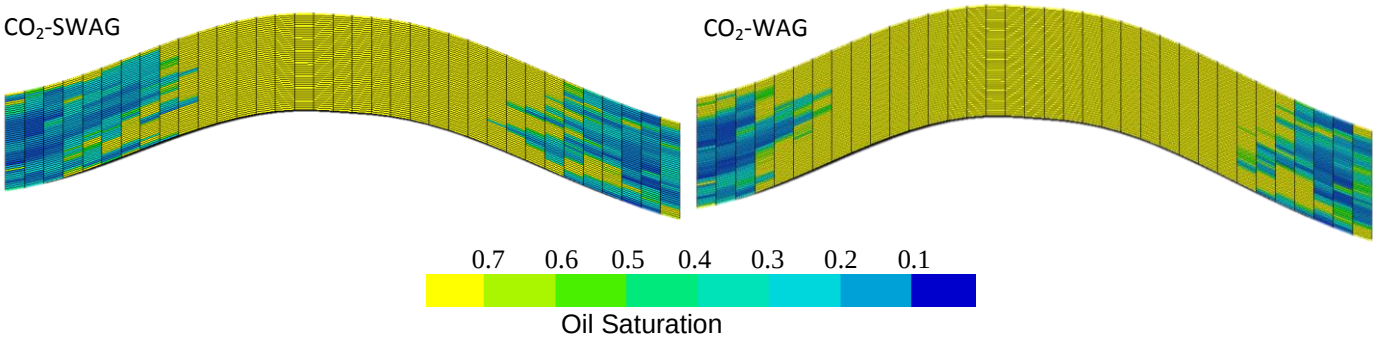

Figure 23 Cross-sectional view of oil saturation for model 2 after two years of EOR

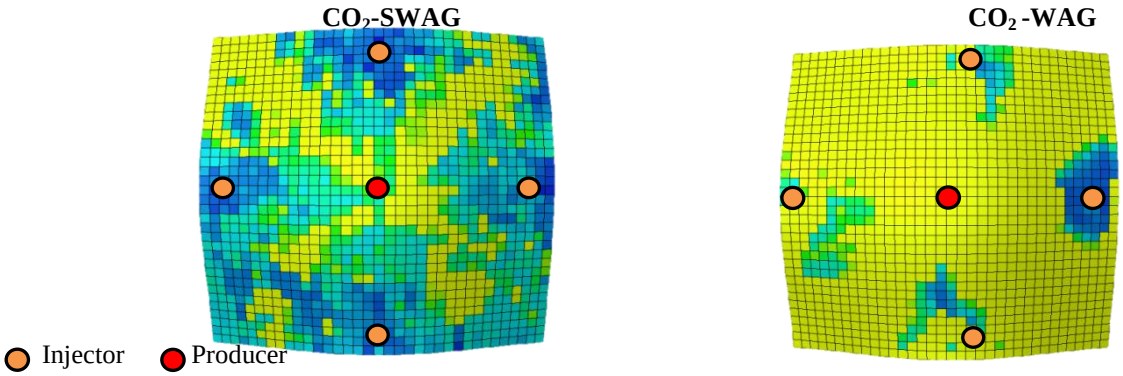

Figure 24 Final oil saturation distribution of SWAG and CO_2-WAG after 20 years of EOR

Discussion

Before conducting our analysis we investigated the impact of grid dimensions when simulating compositional simulation studies. Christensen (1998) recommended a vertical thickness of 0.35-0.7 m and Sifuentes *et al.* (2009) recommendations were to consider a horizontal grid length of 30.5 m. In this paper we used a gridblock dimension of 30.5×30.5×0.7 m.

For the purpose of this study we refined the SPE 5 model with reservoir dimensions of 1067×1067×30m with discretization of 7×7×1 grid cells to 35×35×50. In addition, the fluid model was modified by adding a CO_2 component. Synthetic three-phase relative permeability curves were generated using three-phase relative permeability endpoints from Oak's experiments (Oak, 1990), in order to study gas trapping effects. Larsen and Skauge's three-phase WAG hysteresis model was used in the simulation (Larsen and Skauge, 1998). Simulations were also conducted to study the effects of CO_2 solubility in water using

Chang *et al.* (1998) correlation. The study was extended to analyze SWAG injection for both CO_2 –EOR and sequestration purposes.

The study has shown that the combination of hysteresis and CO_2 solubility has a significant impact on the performance of the reservoir on both small and field scale. Simulations incorporating these effects experienced severe gas injectivity losses, which affected pressure maintenance and oil production rate. The results also demonstrated that CO_2 solubility in water in a SWAG injection strategy had little impact the reservoir performance.

Simulations were performed on regular WAG cycles and varied WAG ratio. In these models, injecting more water than gas resulted in more favourable reservoir performance; higher oil recovery, less CO_2 production and delayed water-cut. These simulation results and observations are in agreement with Qi *et al.* (2008) who showed that traditional CO_2-WAG with optimal WAG ratio is not ideal for coupled CO_2-EOR and Sequestration projects. The impact of CO_2 solubility on CO_2 sequestration was investigated. From the analysis it is evident that CO_2-WAG is more favourable for sequestration, because the injected CO_2 dissolves in accumulated water in the bottom of the formation.

On the other hand, in CO_2-SWAG the CO_2 solubility effects in water were not significant. Gas and water are injected simultaneously in separated perforations. There is less time for CO_2 and water to interact, because both fluids separate very rapidly, with CO2 remaining at the top of the reservoir.

Conclusions

The main conclusions of this study are as follows:

1. The effect of CO_2 solubility in water in a CO_2-WAG EOR strategy, using a WAG hysteresis model is of great importance. It is strongly recommended to include this in simulation models, particularly when the reservoir has been previously waterflooded. The simulation study can predict potential gas injectivity losses, which occur when CO_2 dissolves in the aqueous phase. Injectivity losses decrease pressure maintenance, which can affect the feasibility of a miscible gas injection project.
2. In the heterogeneous reservoir model studied, SWAG provides better mobility contrast and sweep efficiency compared to CO_2-WAG. From an EOR perspective miscible SWAG injection contacts more oil in the reservoir.
3. In this paper we demonstrated in our simulation that including the effects of CO_2 solubility in water for a CO_2-SWAG strategy does not make much difference, because of rapid separation of the CO_2 and water phase.
4. In our study we also demonstrated that injecting more water than CO_2 delays gas and water breakthrough in a homogenous reservoir. A short CO_2 injection periods increases CO_2 trapping.

Recommendations for future study

1. This simulation study was conducted on a sector model. We recommend further studies on a full field model.
2. The effects of a CO_2-EOR simulation study in an aquifer incorporating CO_2 solubility effects in water will be of great importance for real-field studies, e.g. for North Sea reservoirs.
3. For SWAG injection it would be recommended to implement techniques such as chase brine injection after a SWAG injection period.
4. For CO_2 sequestration SWAG processes have to be optimized, in order to delay early gas breakthrough.

Nomenclature

k_{rw}	Water Relative Permeability
$k_{rw(o)}$	Water Relative Permeability in Water-Oil displacement
k_{ro}	Oil Relative Permeability
$k_{ro(w)}$	Oil Relative Permeability in Water-Oil displacement
$k_{ro(g)}$	Oil Relative Permeability in Oil-Gas displacement
k_{rg}	Gas Relative Permeability
$k_{rg(o)}$	Gas Relative Permeability in Oil-Gas displacement
k_{rg}^{drain}	Drainage Gas Relative Permeability
k_{rg}^{imb}	Imbibition Gas relative Permeability
S_w	Water Saturation
S_o	Oil Saturation
S_g	Gas Saturation
S_{wc}	Connate Water Saturation
$S_{or(w)}$	Residual Oil Saturation to Water
$S_{or(g)}$	Residual Oil Saturation to Gas
S_{gc}	Critical Gas Saturation

C	Land trapping coefficient
S_{gt}	Trapped Gas Saturation
$S_{gt,max}$	Maximum Trapped Gas Saturation
S_{gf}	Flowing Gas Saturation
$S_{g,hy}$	Gas Saturation Flow Reversal
α	Secondary Drainage Reduction Exponent

Reference

Blunt, M. J.: "An Empirical Model for Three-Phase Relative Permeability" ,SPEJ, **5** (4), 435-445, December 2000.

Chang, Y-B, Coats B. K., and Nolen, J. S. "A Compositional Model for CO_2 Floods Including CO_2 Solubility in Water," *SPE Journal*, SPE Reservoir Evaluation & Engineering 1 No. 2, 155-160, 1998.

Christensen, J. R., "Compositional and Relative Permeability Hysteresis Effects on Near-Miscible WAG", SPE 39627, proceedings of SPE/DOE Improved Oil Recovery Symposium, 19-22 April, Tulsa, Oklahoma, January 1998.

Christensen, J. R., Stenby, E. H., & Skauge, A.,"Review of WAG Field Experience", SPE 39883, proceedings of International Petroleum Conference and Exhibition of Mexico, 3-5 March, Villahermosa, Mexico, 1998.

Christensen, J. R., Larsen, M., Nicolaisen, H.,"Compositional Simulation of Water-Alternating-Gas Processes". SPE 62999, proceedings of the SPE Annual Technical Conference and Exhibition, 1-4 October, Dallas, Texas, 2000.

Dake, L. P.: Fundamentals of Reservoir Engineering, Elsevier, 1978.

Ghomian, Y., Pope, G. A., & Sepehrnoori, K.,"Hysteresis and Field-Scale Optimization of WAG Injection for Coupled CO2-EOR and Sequestration". SPE 110639, proceedings of the SPE Symposium on Improved Oil Recovery, 20-23 April, Tulsa, Oklahoma, USA, January 2008.

Killough, J. E.: "Reservoir Simulation with History-Dependent Saturation Functions," SPE 5105, proceedings of the SPE-AIME 49th Annual Fall Meeting, held in Houston, October 6-9, 1974.

Killough, J. E., Kossack, C. A.: "Fifth Comparative Solution Project: Evaluation Of Miscible Flood Simulators," paper SPE 16000, proceedings of the Ninth SPE Symposium on Reservoir Simulation held in San Antonio, Texas, February 1-4, 1987.

Kossack, C. A.: "Comparison of Reservoir Simulation Hysteresis Options," paper SPE 63147, proceedings of the 2000 SPE Annual Technical Conference and Exhibition held in Dallas, Texas, 1-4 October 2000.

Krumhansl, J.L., R. Pawar, R. Grigg, H. Westrich, N. Warpinski, D. Zhang, C. Jove-Colon,P. Lichtner, J. Lorenz, R. Svec, B. Stubbs, S., Cooper, C. Bradley, J. Rutledge, and C. Byrer,Geological Sequestration of Carbon Dioxide in a Depleted Oil Reservoir, proceedings of the SPE/DOE 13th Symposium on Improved Oil Recovery, Tulsa, OK, April 13-17, 2002.

Lake, L. W.: Enhanced Oil Recovery, Prentice-Hall, Inc. 1989.

Land, C. S.: "Calculation of Imbibition relative Permeability for Two and Three-Phase Flow from Rock Properties," paper SPE 1942, proceedings of the SPE 42nd Annual Fall Meeting held in Houston, Texas, USA, October 1-4, 1967.

Larsen, J. A., Skauge, A.: "Methodology for Numerical simulation with Cycle-Dependent relative Permeabilities," paper SPE 38456, SPEJ, June 1998.

Oak, M. J., Three-Phase Relative Permeability of Water-Wet Berea. SPE 20183, proceedings of the SPE Annual Technical Conference and Exhibition, 26-29 September, Houston, Texas, January 1990.

Pollack, N.R., et al.: "Effect of an Aqueous Phase on CO_2/Tetradecane and CO_2/Maljamar-Crude-Oil Systems," SPERE, 533, May 1988

Qi, R., LaForce, T. C., & Blunt, M. J., "Design of Carbon Dioxide Storage in Oil Fields". SPE 115663, proceedings of the SPE Annual Technical Conference and Exhibition, 21-24 September, Denver, Colorado, USA, January 2008.

Rogers, J. D., & Grigg, R. B.,"A Literature Analysis of the WAG Injectivity Abnormalities in the CO_2 Process. SPEJ, **4** (5), 375-386, 2001.

Sifuentes, W. F., Giddins, M. A., & Blunt, M. J, "Modeling CO_2 Storage in Aquifers : Assessing the key contributors to uncertainty". SPE 123582, proceedings of the Offshore Europe conference, 8-11 September, Aberdeen, UK, January 2009.

Spiteri, E.J., Juanes, R.: "Impact of Relative Permeability hysteresis on Numerical simulation of WAG Injection," paper SPE 89921, proceedings of the SPE Annual Technical Conference and Exhibition held in Houston, Texas, USA, 26-29 September 2004.

Spiteri, E.J., Juanes, R., Blunt, M.J., Orr, F.M.: "A New Model of Trapping and Relative Permeability Hysteresis for All Wettability Characteristics," paper SPE 96448, SPEJ, September 2008.

Schlumberger Reference Manual and Technical Description, Copyright 2014, Schlumberger, 2014.

Appendix A: Literature Review

Paper	Year	Title	Authors	Contribution
1600	1987	Fifth Comparative Solution Project: Evaluation of Miscible Flood Simulators	Killough, J. E., Kossack, C. A.	Studied the effects of miscibility by using compositional simulators
1942	1981	Calculation of Imbibition Relative Permeability for Two- and Three- Phase Flow From Rock Properties	Land, C. S.	Developed a trapping model for two- and three-phase relative permeability, which is a foundation for most hysteresis models.
5106	1976	Reservoir Simulation With History-Dependent Saturation Functions	Killough, J. E	Developed a two-phase relative permeability hysteresis model, which is widely used in current reservoir simulators.
9992	1983	Status of Miscible Displacement	Stalkup Jr., F. I.	Described the mechanics of First-Contact and Multi-Contact miscibility as well as vaporizing and condensing drive. In addition, he mentioned the advantages of using CO_2 as a gas injection method in the early stages of CO_2 flooding.
10157	1981	Simulation of Relative Permeability Hysteresis to the Nonwetting Phase	Carlson, F. M.	Developed a method where the relative permeability at any saturation can be calculated from the imbibition curve. Carlson also identified that the residual non-wetting phase saturation can be calculated without the need of laboratory specifications of the imbibition curve.
24928	1992	Update of Industry Experience With CO2 injection	Hadlow, R. E	Hadlow addressed the issue injectivity losses of injecting CO_2 and Water for CO_2 WAG purposes.
39626	1998	A Case Study in Scaleup for Multi-contact Miscible Hydrocarbon Gas Injection	Jerauld, G. R.	Described the impact of fine scale resolution to simulate miscible gas injection.
39627	1998	Compositional and Relative Permeability Hysteresis Effects on Near-Miscible WAG	Christensen, J. R.	Identified that recovery by WAG injection process may result in underestimation using compositional models, because inadequate modelling of cycle dependent relative permeability hysteresis.
56474	1999	An Empirical Model for Three-Phase Relative Permeability	Blunt, M. J.	Developed a new empirical model for three-phase relative permeability.

63147	2000	Comparison of Reservoir Simulation Hysteresis Options	Kossack, C. A.	Provided a concise summary of all Hysteresis options used in ECLIPSE.
89921	2004	Impact of Relative Permeability Hysteresis on Numerical Simulation of WAG Injection	Spiteri, E. J., Juanes, R.	Analysed hysteretic and nonhysteretic models for WAG prediction. The identified that hysteresis models take into account the trapping of the non-wetting phase.
96448	2005	Relative Permeability Hysteresis: Trapping Models and Application to Geological CO_2 Sequestration	Spteri, E. J., Juanes, R., Blunt, M. J., Orr Jr., F. M.	Proposed a new model for a range of rock wettability, which accounts trapping and waterflood relative permeability.
99721	2007	Impact of Viscous Fingering on the Prediction of Optimum WAG Ratio	Juanes, R., Blunt, M. J.	They proofed that minimal change in the optimum WAG ratio occurs when viscous fingering effects are included, which was initially proposed by Stalkup (1983). In addition, they demonstrated that the fractional flow theory developed by Walsh and Lake (1989) is unreliable.
109905	2007	Design of Carbon Dioxide Storage in a North Sea Aquifer using Streamline-Based Simulation	Qi, R., Beraldo, V., LaForce, T., Blunt, M. J.	Proposed an injection strategy, which increases CO_2 storage and minimizes Water injection - Injecting CO_2 with fraction flow ranges between 85 to 100%, followed short period of brine injection.
110639	2008	Hysteresis and Field-Scale Optimization of WAG Injection for Coupled CO_2-EOR and Sequestration	Ghomian, Y., Pope, G. A., Sepehrnoori, K.	Demonstrated the importance of coupled CO_2-EOR and Sequestration incorporating the effects of Hysteresis effects.
115663	2008	Design of Carbon Dioxide Storage in Oilfields	Qi, R., LaForce, T. C., Blunt, M.J.	This paper is an extension of Qi et al. in 2007 work. In this study they proposed to inject more water than the optimum WAG ratio for increased CO_2 trapping and extending the reservoir field life. This study provided an innovative solution to trap significant amount of CO_2 using chase brine injection followed by SWAG injection. However, this method was proposed in the previous paper.
123582	2009	Modeling CO_2 Storage in Aquifers: Assessing the Key Contributors to Uncertainty	Sifuentes, W., Blunt, M. J., Giddins, M. A.	Studied the impact on CO_2 dissolution and residual trapping in aquifers.

SPE 1600

Fifth Comparative Solution Project: Evaluation of Miscible Flood Simulators

Authors: Killough, J. E., Kossack, C. A.

Year: 1987

Contribution to the understanding of Miscible Gas Injection:
Studied the effects of miscibility by using compositional simulators

Objective of this paper:
Compare the results of three WAG scenarios using different simulators from the participants (BP, Chevron, CMG, Energy Research Consultants, Reservoir Simulation Research Corp., Todd, Dietrich and Chase Inc.).

Methodology:
Investigate three WAG cases on a four-component fluid model using the compositional simulators from the participants. The WAG duration lasts 20 years.

Case 1:
Oil production at 12,000 bbl/day with Bottom Hole Pressure (BHP) 1000 psi.
WAG is implemented after one year production.
One year WAG cycle starting by injecting Water first at a rate of 12,000 bbl/d followed by Gas injection at a rate of 12,000 Mcf/d with a maximum BHP of 10,000 psi.

Case 2:
Oil production at 12,000 bbl/day with Bottom Hole Pressure (BHP) 3000 psi.
WAG is implemented immediately.
Three months WAG cycle starting by injecting Water first at a rate of 45,000 bbl/d followed by Gas injection at a rate of 20,000 Mcf/d with a maximum BHP of 4500 psi.

Case 3:
Oil production at 12,000 bbl/day with Bottom Hole Pressure (BHP) 1000 psi.
WAG is implemented after two years of production.
One year WAG cycle starting by injecting Water first at a rate of 12,000 bbl/d followed by Gas injection at a rate of 30,000 Mcf/d with a maximum BHP of 4500 psi.

Conclusion:
Results showed that injection rates, which were limited to BHP particular attention should be given to the near-well phase mobility calculations. Three phase relative permeability treatments in the cases near the wells might have affected the results to lower degree.

Comments:
Adapt Reservoir model and refine grid dimension to study the effects of CO_2 WAG.
Also implement similar WAG injection strategy.

SPE 1942

Calculation of Imbibition Relative Permeability for Two- and Three- Phase Flow From Rock Properties

Author: Land, C. S.

Year: 1981

Contribution to the understanding of Hysteresis effects:
Developed a trapping model for two- and three-phase relative permeability, which is a foundation for most hysteresis models.

Objective of this paper:
Formulated an equation for relative permeability expressed as a function of saturation.

Methodology:
The phase saturation is formulated as followed:

$$S_{gt} = S_{gc} + \frac{S_{g,hy} - S_{gc}}{1 + C(S_{g,hy} - S_{gc})}$$

Where S_{gt} is defined as the trapped gas saturation, $S_{g,hy}$ is the gas saturation when flow reversal occurs and C is defined as Land trapping parameter.
C can be further elaborated between bounding curves of drainage and imbibition:

$$C = \frac{1}{S_{gt,max} - S_{gc}} - \frac{1}{S_{g,max} - S_{gc}}$$

Where the maximum gas saturation is $S_{g,max}$ and the maximum trapped gas saturation is $S_{gt,max}$ with respect to the imbibition curve.

Conclusion:
The direction of the wetting-phase relative permeability in imbibition is greater than the direction of the relative permeability for drainage.

A path can be observed when saturation changes; a reversal from drainage to imbibition can be followed by the non-wetting phase, which is depended on the saturation in the drainage direction. A relative permeability path is reversible during saturation changes in an imbibition process.

Land also mentioned on the effects in a water-wet system, which is influenced by the changes and direction of gas saturation, which impacts the gas distribution.

Comments:
Land's trapping parameter is dependent on rock and fluid type.

SPE 5106

Reservoir Simulation With History-Dependent Saturation Functions

Author: Killough, J. E.

Year: 1976

Contribution to the understanding of Hysteresis:
Developed a two-phase relative permeability hysteresis model, which is widely used in current reservoir simulators.

Objective of this paper:
Present a two-phase relative permeability hysteresis and capillary pressure model, which applies for both wetting and non-wetting phase relative permeability following a scanning curve.

Methodology:
In Killoughs Hsyteresis model the normal gas saturation:

$$S_{g,norm} = S^{i}_{g(o)} + \frac{\left(S_g - S_{gt,max}\right)\left(S_{g,max} - S^{i}_{g(o)}\right)}{S_{g,hy} - S_{gt,max}}$$

Where S^{i}_{g} is the gas saturation with respect to the imbibition curve, $S_{gt,max}$ is the maximum gas saturation trapped, $S_{g,hy}$ is the gas saturation at flow reversal.

The relative permeability values are on the imbibition ($k^{i}_{rg(o)}$) and drainage curve $\left(k^{d}_{rg(o)}\right)$, which are defined as followed:

$$k^{i}_{rg}\left(S_g\right) = \frac{k^{i}_{rg(o)}\left(S_{g,norm}\right) k^{i}_{rg(o)} S_{g,hy}}{k^{d}_{rg(o)} S_{g,max}}$$

Conclusion:
It is important to take the effects of gas trapped into account for water injection, particularly if free gas saturation is present before applying hysteresis on a non-water-wet system.

Comments:
When selecting this option in ECLIPSE reservoir simulators for an imbibition process the Land's constant C is treated independently in the simulation.

SPE 9992

Status of Miscible Displacement

Author: Stalkup Jr., F. I.

Year: 1983

Contribution to the understanding of Miscible & Immiscible CO_2 Gas Injection:
Described the mechanics of First-Contact and Multi-Contact miscibility as well as vaporizing and condensing drive. In addition, he mentioned the advantages of using CO_2 as a gas injection method in the early stages of CO_2 flooding.

Objective of this paper:
Provided a detailed study on miscible gas injection process from previous Laboratory analysis and Field projects.

Methodology:
Stalkup investigated and compared phase behaviour, miscibility, sweep and displacement efficiency and field tests.

Conclusion:
Suggested at that time further research is needed in low temperature CO_2 flooding with miscibility effects, improve understanding using CO_2 injection as tertiary recovery, slug process in order to select miscible and immiscible drive fluids.

In this paper he concluded that the greatest field success were accomplished by vaporizing-gas drives, due to the fact that continuous miscible injection has been implemented as opposed to slug injection. This has achieved a more favourable mobility ratio. However the pressure condition to achieve mobility is high.

Comments:
Fundamental paper on miscible CO_2 injection.

SPE 10157

Simulation of Relative Permeability Hysteresis to the Nonwetting Phase

Author: Carlson, F. M.

Year: 1981

Contribution to the understanding of Hysteresis effects:
Developed a method where the relative permeability at any saturation can be calculated from the imbibition curve. Carlson also identified that the residual non-wetting phase saturation can be calculated without the need of laboratory specifications of the imbibition curve.

Objective of this paper:
Demonstrate the use of parallel imbibition curves.

Methodology:
The formulation of Carlson's method was generated by utilizing a drainage curve, the historical maximum non-wetting phase saturation, minimum point on the imbibition curve and Land's trapping coefficient.

Conclusion:
Carlson's method generates scanning curves which follow parallel to the imbibition curve. The imbibition curves are shifted towards the drainage curve until the imbibition curve intersects the drainage curve at the saturation $\boldsymbol{S_{hy}}$.

Comments:
Carlson's method has the same view as Killough's method on hysteresis effects to the non-wetting phase. Applying this method in a reservoir simulation, it is important that the imbibition curve is steeper than the curve for a given point. If this is not ensured, the scanning curve will cross the drainage curve producing negative $\boldsymbol{S_{ncrt}}$ values.

SPE 24928

Update of Industry Experience With CO_2 injection

Author: Hadlow, R. E

Year: 1992

Contribution to the understanding of CO_2 Injection:
Hadlow addressed the issue injectivity losses of injecting CO_2 and Water for CO_2 WAG purposes.

Objective of this paper:
Provided a brief overview of previous CO_2 injection projects for the last two decades.

Methodology:
Analysed real field CO_2 injection projects and described the benefits and challenges associated with CO_2 injection.

Conclusion:
Comparing all CO_2 projects dating back to the 80's, CO_2 injection provided significant increase in oil production. An average of 20% of injectivity losses has been experienced. Several other issues has been addressed such as early breakthrough and high CO_2 production. It was evident at that time that CO_2 injection has great benefits, which will play an important role in the present and future.

Comments:
Further research is required to understand injectivity loss using CO_2 WAG.

SPE 39626

A Case Study in Scaleup for Multi-contact Miscible Hydrocarbon Gas Injection

Author: Jerauld, G. R.

Year: 1998

Contribution to the understanding of miscible gas injection:
Described the impact of fine scale resolution to simulate miscible gas injection.

Objective of this paper:
Investigate fine grid and scaled up grid for miscible gas injection.

Methodology:
A reservoir with well spacing of roughly 2000 ft with 150 ft total sand thickness. The finest model has 124 layers, which ranged between one to two feet.

Conclusion:
The accuracy of miscible injection in a reservoir simulation is dependent on the grid resolution. Jerauld proposed using tracer response to rank the performance efficiently.

Using pseudo functions from a fine grid will increase the number of relative permeability curves, which will be simplified and become unreliable. Instead history-matched functions are recommended as pseudo functions.

Comments:
In Fine Grid set vertical layering about 1-2 feet and 100ft horizontal layering, which was recommended in Sifuentes et al. (2009).

SPE 39627

Compositional and Relative Permeability Hysteresis Effects on Near-Miscible WAG

Author: Christensen, J. R.

Year: 1998

Contribution to the understanding of Hysteresis effects:
Identified that recovery by WAG injection process may result in underestimation using compositional models, because inadequate modelling of cycle dependent relative permeability hysteresis.

Objective of this paper:
Modelled compositional effects on near-miscible WAG injection for a North Sea oil field.

Methodology:
In this study a sector model was utilized using a black oil-model, which was adjusted accordingly to match the compositional simulation. For the WAG analysis three phase relative permeability hysteresis models from Killough and Carlson were used.

The depth of the reservoir is approximately 2800-3000m containing light oil with a 2 degree dipping angle. The minimum miscibility pressure was obtained via slim tube at 320 bar. The gird was discretized to 20x20x6.

Conclusion:
For the compositional simulations the conclusions were; WAG injection achieves higher recovery, when using wet-gas better recovery cn be accomplished. Tuning the oil, particularly oil viscosity is highly important. Slug size have little impact as opposed to the GOR ratio when implementing WAG. High G/W ratio provides best performance. Incorportaing Killough or Carlsons hysteresis model did not have any influence on WAG performace, oil recovery and breakthrough.

For the black-oil simulations the conclusions were; black-oil model integrated vaporised oil in gas and dissolved gas in oil, because of the significant effects compositional demonstrated. The three phase WAG hysteresis models increased CPU time significantly. However, three-phase WAG hysteresis models increased oil recovery and delayed gas breakthrough. Substantial reduction in gas relative permeability for the three-phase of the reservoir has been identified. Land's trapping constant has not a great impact on simulation results.

Christensen recommended using a three phase WAG hysteresis models with compositional simulation, which would provide better estimates of the combined fluid and compositional effects of oil recovery.

Comments:
Compared both black-oil and compositional fluid model. The MMP could not be obtained from the EOS fluid simulator. Focused only on two hysteresis models – Killough and Carlson.

SPE 56474

An Empirical Model for Three-Phase Relative Permeability

Author: Blunt, M. J.

Year: 1999

Contribution to the understanding of three-phase relative permeability:
Developed a new empirical model for three-phase relative permeability.

Objective of this paper:
Demonstrate a new empirical three-phase relative permeability model, which over comes the limitations from Stone's method.

Methodology:
In this paper a detailed literature review on existing three-phase relative permeability models has been conducted.

The new model is an extension of saturation-weighted interpolation to include oil layer drainage and trapping effects for both oil and gas. In addition, the new model is able to predict three-phase relative permeability path, reservoir wettability and hydrocarbon composition for single and two-phase measurements.

Conclusion:
From previous literature reviews it was identified that Baker's Saturation-weighted interpolation is better in comparison to Stone's Method.

Comments:
Very detailed and concise literature review of exiting relative permeability interpolation models.

SPE 63147

Comparison of Reservoir Simulation Hysteresis Options

Author: Kossack, C. A.

Year: 2000

Contribution to the understanding of Hysteresis:
Provided a concise summary of all Hysteresis options used in ECLIPSE.

Objective of this paper:
Demonstrate all Hysteresis options used in ECLIPSE and explain the physical effects on reservoir simulations.

Methodology:
Models analysed were; Carlsons drainage model (0), Carlsons imbibition model (1), Killough drainage model (2), Killough imbibition model (3), Killough Hysteresis model (4) and the WAG Hysteresis model proposed by Larsen and Skauge.

The simulation was conducted on a simple water-wet linear grid with an example relative permeability data. Five to six WAG cycles were performed in his simulation.

Conclusion:
It is important to have adequate imbibition and drainage curves with the right orientation. In this paper a demonstration is provided on how to develop scanning curves. A detailed WAG displacement was compared and explained.

Comments:
Further information can be obtained from Schlumberger on his work.

SPE 89921

Impact of Relative Permeability Hysteresis on Numerical Simulation of WAG Injection

Authors: Spiteri, E. J., Juanes, R.

Year: 2004

Contribution to the understanding of WAG Hysteresis:
Analysed hysteretic and nonhysteretic models for WAG prediction. The identified that hysteresis models take into account the trapping of the non-wetting phase.

Objective of this paper:
Investigated the influence of history-depended saturation functions in reservoir simulations.

Methodology:
Analysed Oak's three phase relative permeability data from SPE 20183 on different interpolation model to check for their validity. The relative permeability data was incorporated in a 2D homogenous model and the PUNQ-S3 Reservoir model. A sensitivity study was performed on the interpolation models on hysteretic and nonhysteretic simulations for different WAG scenarios.

Conclusion:
In WAG injection incorporating hysteresis effects is of great importance for an appropriate simulation. Two-Phase hysteresis models take the trapping of the non-wetting phase into account but do not imitate the irreversibility of scanning curves.

In WAG simulations gas followed by water injection tend to overestimate the gas relative permeability. During a secondary drainage process, extended models do not take the gas mobility reduction into account. It was highlighted in this paper that most hysteretic models are based on Land's theory, hence Land's coefficient is a key influence for the trapping of the non-wetting phase saturation for a flow reversal process.

This paper demonstrates with a decreasing Land's trapping coefficient the trapping and interfacial tension increases amongst the fluids whilst the permeability of the medium is decreasing.

Additional findings from this paper showed that three-phase hysteresis simulations achieve a higher recovery as opposed to nonhysteretic simulations, because during water flooding a reduction of the mobility of the trapped gas phase is taken into account.

The results of the interpolation model showed higher recovery efficiency, which was tested and validated in the PUNQ-S3 model.

Conclusion:
Oak's permeability data was used for the purpose of this study. Provided summary of many interpolation models and described briefly the hysteresis models.

SPE 96448

Relative Permeability Hysteresis: Trapping Models and Application to Geological CO_2 Sequestration

Authors: Spteri, E. J., Juanes, R., Blunt, M. J., Orr Jr., F. M.

Year:

Contributions to the understanding of Hysteresis simulations:
Proposed a new model for a range of rock wettability, which accounts trapping and waterflood relative permeability.

Objective of this paper:
Emphasized the importance of incorporating CO_2 trapping for the prediction of CO_2 phase mobility and distribution in the reservoir.

Methodology:
The trapping model is able to replicate a non-monotonic behaviour by expressing the oil saturation trapped ($\boldsymbol{S_{ot}}$) as a quadratic equation $\boldsymbol{S_{ot} = \alpha S_{oi} - \beta S_{oi}^2}$, $\boldsymbol{\alpha}$ and $\boldsymbol{\beta}$ represent the initial slope and curvature, which is valid in the ranges of $\boldsymbol{0 \leq \alpha \leq 1}$ and $\boldsymbol{\beta \geq 0}$. The waterflood permeability ($\boldsymbol{k_{ro}^i}$) is calculated at the actual oil saturation ($\boldsymbol{S_o}$), similarly the drainage relative permeability $\left(\boldsymbol{k_{ro}^d}\right)$ is calculated at the flowing saturation $\left(\boldsymbol{S_{of}}\right)$. The flowing saturation is defined as followed:

$$\boldsymbol{S_{of} = \frac{1}{2\beta}\left[(\alpha - 1) + \sqrt{(\alpha - 1)^2 + 4\beta[S_o - S_{ot} + \gamma(S_o - S_{ot})(S_o - S_{oi})]}\right]}$$

where $\boldsymbol{\gamma}$ is a parameter with regards to film flow.

A pore-scale modelling of trapping the hysteresis were performed using the simulator developed by Valvatne and Blunt, which measured advancing contact angle on a rough surface, as function of intrinsic contact angle on a smooth surface.

A simulation was conducted on the PUNQ-S3 model, which was slightly modified for CO_2 injection simulation incorporating hysteresis effects.

Conclusion:
This paper demonstrated that CO_2 trapping can be improved by CO_2 WAG and by operating at high injection rates.

After injection came to halt, CO_2 trapping occurs during upwards migration and displacement of water in the reservoir. As a result residual CO_2 is left behind.

Comments:
Analysis did not include CO_2 dissolution in water. Study included contact angles for wettability analysis.

SPE 99721

"Impact of Viscous Fingering on the Prediction of Optimum WAG Ratio"

Authors: Juanes, R., Blunt, M. J.

Year: 2007

Contribution to the understanding of EOR:
They proofed that minimal change in the optimum WAG ratio occurs when viscous fingering effects are included, which was initially proposed by Stalkup (1983). In addition, they demonstrated that the fractional flow theory developed by Walsh and Lake (1989) is unreliable.

Objective of this paper:
Demonstrated the advantages of injecting more solvent, which the degree minimised fingering.

Methodology:
Analysed a 1D model with a two-phase model constituting three components. The simulation of the fluid flow was analysed for first-contact miscibility (FCM) in which macroscopic viscous fingering effects were taken into account.

Conclusion:
Estimating the optimum WAG ratio including viscous fingering effects are lower that those without fingering. In contrast to Salkup's method, injecting more solvent will lead to a lower PVI. This also defeats the proposal of the fractional-flow theory from Walsh and Lake (1989).

A reemphasis on Blunt and Christi (1993) work on Todd and Longstaff parameter ω was stressed that there is a discontinuity at the optimum WAG ratio. In this paper it is proposed to monotonically and continuously vary ω with the fraction injected but also sustain low values of ω.

Moreover, in this paper an explanation was provided for the solution, which has two solvent fronts, hence two mobility contrast values were provided. The injected mixture constituting more solvent travels with a fast solvent front. An increased fraction of injected water a cross over tales place slowing down the front.

Reasoning for a slower solvent front for a near optimum WAG ratio is that the mobility contrast is lower as opposed to the minimal mobility ratio. Therefore the recommendation is to inject more solvent than initially proposed by Stalkup (1983).

Comments:
This paper is an extension of previous athours. Important papers linked with this publications are; Blunt and Christie (1993[1], 1994[2]), Juanes and Lie (2005[3], 2007[4]), Koval (1963).

[1] Blunt, M. J. and Christie, M. (1993). How to predict viscous fingering in three component flow. *Transp. Porous Media* **12:** 207-236.
[2] Blunt, M. J. and Christie, M. (1994).Theory for Viscous Fingering in Two-Phase, Three-Component Flow. *SPE Advanced Technology series* **2** (2)**:** 52-60.
[3] Juanes, R. and Lie, K.-A. (2005). A Front-Tracking Method for Efficient Simulation of Miscible Gas Injection Processes. Paper SPE 93298 proceedings of the SPE Reservoir Simulation Symposium, The Woodlands, Texas, 31 January–2 February. DOI: 10.2118/93298-MS.
[4] Juanes, R. and Lie, K.-A. (2007). Numerical modeling of multiphase first- contact miscible flows. Part 1. Analytical Riemann solver. Transp. Porous Media 67 (3): 375–393. DOI: 10.1007/s11242-006-9031-1.

SPE 109905

Design of Carbon Dioxide Storage in a North Sea Aquifer using Streamline-Based Simulation

Authors: Qi, R., Beraldo, V., LaForce, T., Blunt, M. J.

Year: 2007

Contribution to the understanding of CO_2 injection:
Proposed an injection strategy, which increases CO_2 storage and minimizes Water injection - Injecting CO_2 with fraction flow ranges between 85 to 100%, followed short period of brine injection.

Objective of this paper:
The main aim for this paper is for CO_2 trapping for Carbon Capture and Storage purposes but it is applicable CO_2 WAG injection studies.

Methodology:
Investigated CO_2 injection using a simulator based on Batycky et al., which was modified later by Obi and Blunt (2006) to incorporate dissolution and dispersion effects of CO_2.

In this paper, relative permeability and trapping model with hysteresis efects were integrated, Contact angles for CO_2 injection were analysed, a One-dimensional results and analytical solutions were obtained, the CO_2 injection was tested on the tenth comparative solution model (SPE 10).

Conclusion:
Successfully demonstrated that injecting CO_2 and brine simultaneously followed by chase brine injection, results in reduces the mobility contrast between CO_2 and brine leading to increased storage efficiency of CO_2.

Qi et al. demonstrated an approach to verify 1D and 3D streamline-based simulation with integrated trapping and relative permeability hysteresis from pore-scale modelling, which were based on experimental measurements.

Suggestion was to inject the largest fractional flow of CO_2 to achieve a good mobility contrast followed by chase brine injection, which increases CO_2 storage.

SPE 110639

Hysteresis and Field-Scale Optimization of WAG Injection for Coupled CO_2-EOR and Sequestration

Authors: Ghomian, Y., Pope, G. A., Sepehrnoori, K.

Year: 2008

Contribution to the understanding of CO_2-EOR:
Demonstrated the importance of coupled CO_2-EOR and Sequestration incorporating the effects of Hysteresis effects.

Objective of this paper:
Analyse and provide an understanding of the most influential factors effecting oil recovery, economics of a project and CO_2 storage within a reservoir.

Methodology:
Conducted an analysis on 2D dipping and 3D compositional simulations. The fluid in place is light oil, which was generated in a compositional EOS simulator. A Slim-tube simulation was performed to determine the minimum miscibility pressure (MMP). A grid refinement study was performed for convergence purposes. In this study simulations were performed with and without hysteresis effects using three different relative permeability and capillary models. CO_2 WAG injection was performed including variations of CO_2 slug sizes and WAG ratios.

Conclusion:
The main conclusion of this paper is that Hysteresis effects have significant impact on both oil recovery and CO_2 Storage. Hysteresis is key for trapping CO_2 in the formation. It is important to incorporate residual gas for the global CO_2 stored within an oil reservoir. The study has identified that the most significant aspect effecting CO_2 Storage are WAG ratios, WAG ratio including Hysteresis and CO_2 Slug size. In this paper it is recommended that oil reservoirs with low heterogeneity the CO_2 storage is greater when high WAG ratio and large CO_2 slug sizes are considered.
In terms of oil recovery, more oil is recovered because of the mobility ratio and improved sweep efficiency.

Comments:
Methods were proposed to mitigate early gas breakthrough. However, this study did not take CO_2 solubility into account.

SPE 115663

Design of Carbon Dioxide Storage in Oilfields

Authors: Qi, R., LaForce, T. C., Blunt, M.J.

Year: 2008

Contribution to the understanding of CO_2 injection:
This paper is an extension of Qi et al. in 2007[5] work. In this study they proposed to inject more water than the optimum WAG ratio for increased CO_2 trapping and extending the reservoir field life. This study provided an innovative solution to trap significant amount of CO_2 using chase brine injection followed by SWAG injection. However, this method was proposed in the previous paper.

Objective of this paper:
Analyse oil production and CO_2 storage in reservoirs using streamline based simulation, which captures the effects of CO_2 dissolution, dispersion, gravity and chemical reactions.

Methodology:
This study included a 1D simulation and the SPE 10^{th} comparative 3D reservoir model. The analysis was conducted using streamline based simulation to investigate the effects of CO_2 storage in oilfields. The relative permeability data was taken from the Berea Sandstone based on Oak (1990) paper. The imbibition and drainage curve were based on Spierie et al. (2005).

Conclusion:
This study recommends SWAG injection of Water and CO_2 to increase CO_2 Storage within an oil reservoir. In their extended study it was highlighted to inject more water than the estimates optimum value. This will allow the water front to move ahead of the CO_2, which will retain the CO_2 at low saturation and immobile in the reservoir.

Furthermore, chase brine injection will trap or dissolve the CO_2 increasing the storage efficiency.

Comments:
The analysis took CO_2 dissolution into account. The dataset for relative permeability was taken from Oak (1990). The imbibition and drainage curve were obtained from Spierie et al. (2005). These information will be used for this research project.

[5] Qi, R., Beraldo, V, LaForce, T. C. and Blunt, M. J. (2007). Design of Carbon Dioxide Storage in a North Sea Aquifer using Streamline-based Simulation, SPE 109905

SPE 123582

Modeling CO_2 Storage in Aquifers: Assessing the Key Contributors to Uncertainty

Authors: Sifuentes, W., Blunt, M. J., Giddins, M. A.

Year: 2009

Contribution to the understanding CO_2 injection:
Studied the impact on CO_2 dissolution and residual trapping in aquifers.

Objective of this paper:
Investigate the effectiveness of CO_2 storage in aquifers by conducting sensitivity analysis using experimental design to determine parameters effecting CO_2 trapping.

Methodology:
A simple homogenous 3D grid was constructed to isolate the contribution of the parameters. Later heterogeneity was introduced. The relative permeability curves were based on Brooks-Corey equations. In this simulation Killough's Hysteresis method has been utilized.

The study was then extended to the pilot geological storage project CO2SINK. The fluid property was highly saline and the CO2 was injected for 40 years.

In this paper temperature, brine salinity, horizontal permeability, pressure, dipping angle, Heterogeneity, Hysteresis, Injection strategy, Well completions and Multiparameter effects were studied.

Conclusion:
The main contributor is horizontal permeability, which effects residual trapping and solubility. High permeability is responsible for fast CO_2 migration in the top of the reservoir.

It is crucial to take hysteresis effects into account, which was first identified by Juanes et al. (2006)[6]. Using just the imbibition curve will over predict the total amount CO_2 residual. On the other hand just using the drainage curve will underestimate the total amount of residual CO_2. It is important to note that gas saturation is sensitive to the residual gas saturation. Moreover, during WAG injection forced imbibition is improves residual trapping mechanism.

According to Ennis-King and Paterson (2005)[7] gravity segregation and convective mixing are important aspects to capture these effects very fine grid cells are essential. Coarse gridblocks underestimate the total amount of CO_2 dissolved.

Comments:
Recommended horizontal width of grid cells are 33m ~100ft.

[6] Juanes, R., Spiteri, E. J., Orr Jr., F.M. and Blunt, M. J.:"Impact of relative permeability hysteresis on geological CO2 storage", Water Resources Research, **42**, W12148, doi: 10.1029/2005wr004806, (2006).
[7] Ennis-King, J. and Paterson, L.:" Role of convective mixing in the long-term storage of carbon dioxide in deep saline aquifers", *SPEJ* **10** (3), 349-356, (2005).

Appendix B: Fluid Model

Fig. 25 illustartes the phase envelope. The reservoir temperature is 71 degrees and intial reservoir pressure is

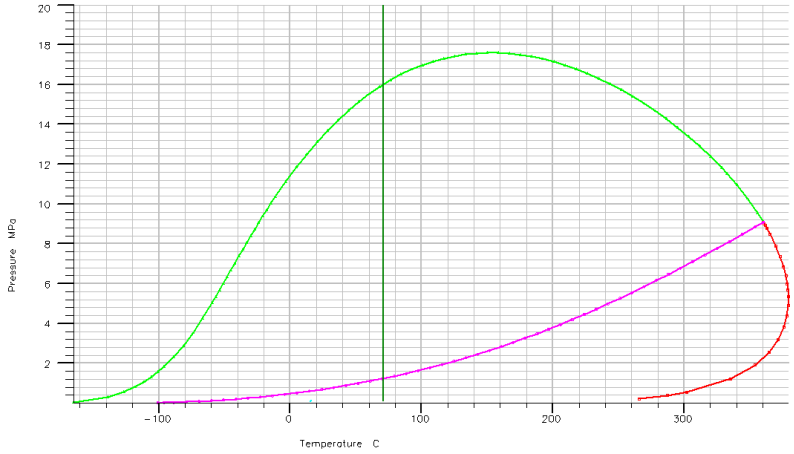

Figure 25 Phase Diagram at bottom hole pressure constraint of 17.2 MPa at reservoir temperature of 71 degrees Celsius

Fig. 26 shows the ternary plot of the fluid model at 17.2 MPa with reservoir temperature of 71 degrees Celsius.

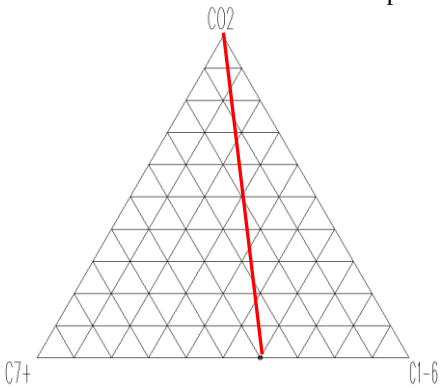

Figure 26 Ternary plot of Fluid at 17.2 MPa with reservoir temperature at 71 C

In **Fig.27** a slimtube simulation was performed the MMP has been identified at 16.5 MPa.

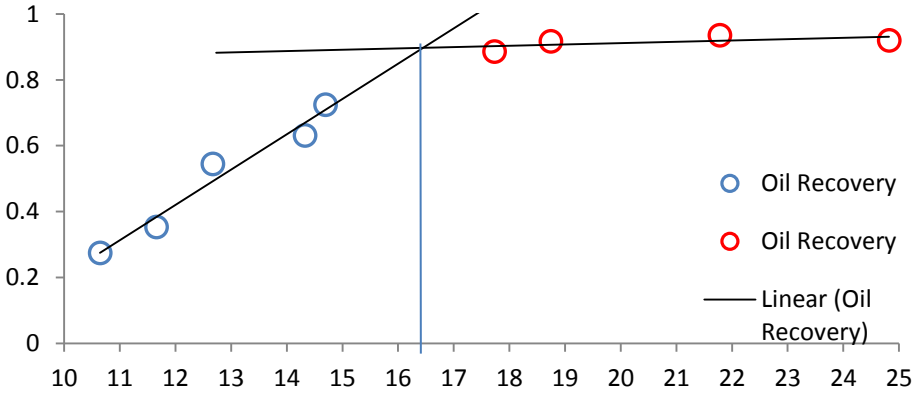

Figure 27 Slimtube Simulation to determine the Minimum Miscibility Pressure (MMP) of the compositional Fluid model

Appendix C: Heterogenous model

In **Tabel 7** a summary of the hetertogenous properties is provided and in **Fig. 28** varying rock types.

Heterogeneous Model				
Rock Type	**Porosity**	**Permeability XY (mD)**	**Permeability Z (mD)**	**kv/kh**
1	18%	120	15.6	0.13
2	25%	1000	120	0.12
3	16%	40	6	0.15
4	11%	1	0.11	0.11
5	5%	0.1	0.013	0.13

Reservoir Layer	**average Porosity**	**average kxy (mD)**	**average kz (mD)**
Layer 1	0.14	125	16
Layer 2	0.17	319	39
Layer 3	0.14	224	27

Table 7 Summary of Heterogeneous properties.

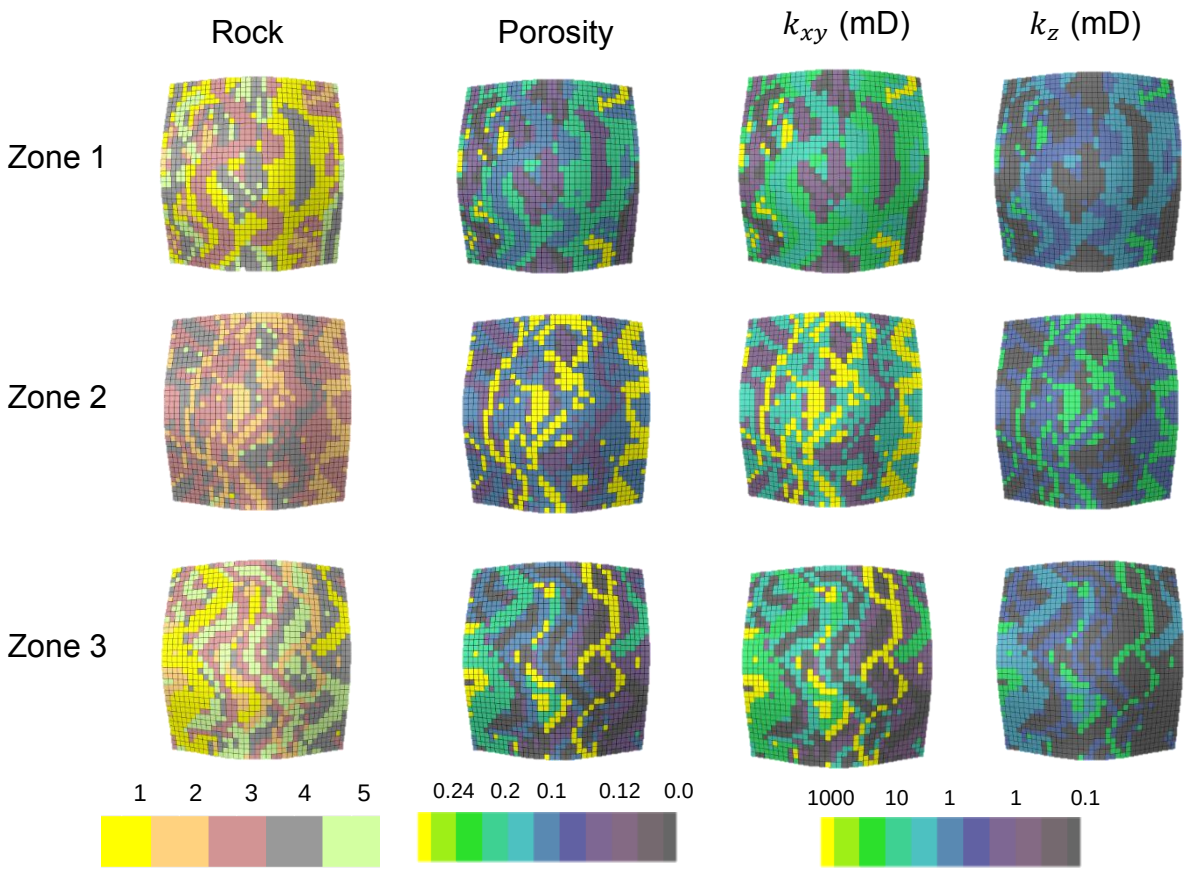

Figure 28 Heterogenous Model using Model 2 with varying porosity and permeability distribution

Appendix D: ECLIPSE E300 Keywords

Keyword	Description
MISCIBLE	Activates miscible flooding using Todd-Longstaff treatment
CO2SOL	Activates CO_2 solubility in aqueous phase using Chang et al. (1998) correlation
HYSTER	Enables hysteresis option
SALINITY	Molality of the reservoir fluid can be fined
SOLUBILI	Water salinity with respect to pressure can be defined
EHYSTR	Enables to use Hysteresis option (Carlson, Killouh, Jargon) for wetting and non-wetting phase
WAGHYSTR	Activates Larsen and Skauge WAG hysteresis (1998) option
SATNUM	Defines the cells to use the drainage curve
IBNUM	Defines the cells to use the imbibition curve
WH2NUM	Defines the cells to use two-phase curve
WH3NUM	Defines the cells to use three-phase curve